Stanford Geothermal Program
Interdisciplinary Research
in Engineering and Earth Sciences
Stanford University
Stanford, California

THE EFFECTS OF TEMPERATURE AND PRESSURE ON ABSOLUTE PERMEABILITY OF SANDSTONES

by
Muhammadu Aruna

April 1976

This research was carried out
under Research Grant GI-34925
by the National Science Foundation

ACKNOWLEDGEMENT

The author would like to express his sincere appreciation to his adviser, Dr. Henry J. Ramey, Jr., for his instruction and guidance throughout the research work. He made it possible for the author to come to Stanford University and complete his graduate studies successfully.

The assistance and practical suggestions from the faculty of the Department of Petroleum Engineering, particularly from Dr. W. E. Brigham and Dr. Sullivan S. Marsden, are gratefully acknowledged. The cooperation I enjoyed from the department secretaries, especially from Alice Mansourian, will not be forgotten.

Many thanks are due to my friends, particularly Norio Arihara, H. K. Chen, and Paul Atkinson, for their helpful comments and timely help through the days of experimental work.

Credit for modification of the apparatus built by Weinbrandt and Cassé is due Jon Grim, the Petroleum Engineering Department machinist.

Finally, Dr. F. Cassé reviewed this manuscript and made many helpful suggestions.

This work was funded under National Science Foundation Grant No. GI-34925.

This report was prepared originally as a dissertation submitted to the Department of Petroleum Engineering and the Committee on the Graduate Division of Stanford University in partial fulfillment of the requirements for the degree of Doctor of Philosophy.

DEDICATED TO MY PARENTS AND

ALL THE GOOD PEOPLE IN MY LIFE

ABSTRACT

The standard procedure for determining the permeability of porous media according to API Code No. 27 is based on the fundamental assumption that, as long as viscous flow prevails, the absolute permeability of a porous medium is a property of the medium, and is independlent of the fluid used in its determination, slip effect being taken into account in the case of gas flow. Absolute permeability has, therefore, been traditionally measured at room conditions, with the assumption that it changes only with overburden pressure and not with temperature. Results obtained at room temperature may then be used to predict performance at reservoir conditions after correction for reduction by stress effects.

Although this assumption is true for most fluids, results of recent absolute permeability measurements of water flow through porous media at high temperatures[1,16] and high overburden pressures differ from room condition values. Not only was the absolute permeability to water at high confining pressure lower than that to other fluids used at room temperature, but also, there was a significant permeability reduction at elevated temperatures.

An existing permeameter was modified to enable flow of different fluids through separate flow lines. Distilled water, a white mineral oil, nitrogen and 2-octanol were the

fluids used, and tests were carried out on natural consolidated sandstones and unconsolidated silica sand.

With the exception of water, the absolute permeabilities of the cores to other fluids showed little or no temperature dependence. The reduction in permeability to water with temperature increase was attributed to interaction between water and silica. In the case of water flow through geothermal systems or in thermal recovery processes which cause large changes in formation temperatures, the effect of temperatures on absolute permeability should be considered in engineering calculations.

TASLE OF CONTENTS

		Page
ACKNOWLEDGEMENT		iv
ABSTRACT,		v
TABLE OF CONTENTS		vii
LIST OF TABLES.		x
LIST OF FIGURES		xi
CHAPTERS		
1.	INTRODUCTION.	1
2.	FLOW IN POROUS MEDIA.	4
	2.1 Darcy's Law.	4
	2.2 Darcy's Law for Gas Flow	5
	2.3 Slip Phenomena in Gas Flow	6
	2.4 Visco-Inertial Flow.	7
3.	LITERATURE.	9
4.	EXPERIMENTAL EQUIPMENT.	15
	4.1 General Description.	15
	4.2 Core Holder.	18
	4.3 Air Bath and Temperature Control	18
	4.4 Liquid and Gas Sources	20
	4.5 Liquid Pumps	21
	4.6 Hydraulic Hand Pump.	21
	4.7 Heat Exchangers.	21

Table of Contents, continued

		Page
4.8	Backpressure Valve	22
4.9	Flow Rate Measuring Devices	22
4.9-1	Liquid Flow	22
4.9-2	Gas Flow	23
4-10	Pressure Recording Devices	23
5.	PROCEDURE	25
5.1	Core Preparation	25
5.1-1	Consolidated Massillon Sandstones	25
5.1-2	Unconsolidated Ottawa Sand	26
5.2	Establishing Run Conditions	27
5.3	Measurements and Calculations	28
5.3-1	Liquid Flow	28
5.3-2	Gas Flow	37
6.	ANALYSIS OF RESULTS AND DISCUSSION	41
6.1	Water Flow	41
6.1-1	Consolidated Sandstones	41
6.1-2	Unconsolidated Sand	43
6.2	Gas Flow	48
6.2-1	Consolidated Sandstones	50
6.2-2	Unconsolidated Sand	56
6.3	Oil Flow	56
6.4	2-Octanol Flow	58
6.5	Discussion	62
7.	CONCLUSIONS AND RECOMMENDATIONS	65
8.	REFERENCES	67

Table of Contents, continued

		Page
9.	APPENDICES.	70
	9.1 List of Tabulated Data	**71**
	9.2 Core Data.	90
	9.3 Derivations of Equations	94
	9.4 List of Manufacturers.	99
10.	NOMENCLATURE.	**102**

LIST OF TABLES

Table		Page
1	Density and Viscosity of Water vs. Temperature	72
2	Viscosity of Nitrogen vs. Temperature	73
3	Viscosity of Chevron Oil No. 3 vs. Temperature	74
4	Density of 2-Octanol vs. Temperature.	75
5	Viscosity of 2-Octanol vs. Temperature.	76
6	Flow Data for Massillon Sandstone Core No. 2, Water Flow.	77
7	Flow Data for Massillon Sandstone Core No. 3, Water Flow.	78
8	Flow Data for Massillon Sandstone Core No. 4, Water Flow.	80
9	Flow Data for Massillon Sandstone Core No. 5, Nitrogen Flow	81
10	Flow Data for Massillon Sandstone Core No. 6, Nitrogen Flow	82
11	Flow Data for Massillon Sandstone Core No. 10, Oil Flow.	84
12	Flow Data for Massillon Sandstone Core No. 11, Oil Flow.	85
13	Flow Data for Unconsolidated Ottawa Silica Sand Core No. 14, Water Flow.	86
14	Flow Data for Unconsolidated Ottawa Silica Sand Core No. 15, Water Flow.	87
15	Flow Data for Unconsolidated Ottawa Silica Sand Core No. 16, Nitrogen Flow and Water Flow..	88
16	Flow Data for Unconsolidated Ottawa Silica Sand Core No. 17, 2-Octanol Flow.	89

LIST OF FIGURES

Figure		Page
1	Photograph of Apparatus	16
2	Details of Assembly in the Air Bath	16
3	Schematic Diagram of Apparatus.	17
4	Schematic Diagram of the Core Holder.	19
5	Density of Water vs. Temperature of 200 psig	31
6	Water Viscosity vs. Temperature at 200 psig	32
7	Density vs. Temperature for Chevron White Oil No. 3 at 14.7 psi	33
8	Viscosity vs. Temperature for Chevron White Oil No. 3	34
9	Density of 2-Octanol vs. Temperature at 14.7 psi	35
10	Viscosity of 2-Octanol vs. Temperature.	36
11	Viscosity of Nitrogen vs. Temperature	39
12	Water Permeability vs. Temperature, Massillon Sandstone Core No. 2.	42
13	Water Permeability vs. Temperature, Massillon Sandstone Core No. 3.	44
14	Water Permeability vs. Temperature at a Constant Confining Pressure of 3000 psig, Massillon Sandstone Core No. 3.	45
15	Water Permeability vs. Temperature, Massillon Sandstone Core No. 4.	46
16	Water Permeability vs. Temperature, Unconsolidated Ottawa Silica Sand Core No. 14.	47
17	Water Permeability vs. Temperature, Ottawa Silica Sand Core No. 15	49

List of Figures, continued

Figure		Page
18	Apparent Permeability vs. Reciprocal Mean Pressure at Several Temperatures for Massillon Core No. 5.	51
19	Modified Visco-Inertial Graph, Massillon Core No. 5 with Nitrogen Flow	52
20	Apparent Permeability vs. Reciprocal Mean Pressure at Several Temperatures for Massillon Sandstone Core No. 6, Confining Pressure = 1000 psig	53
21	Apparent Permeability vs. Reciprocal Mean Pressure at Several Temperatures for Massillon Sandstone Core No. 6, Confining Pressure = 3000 psig.	54
22	Apparent Permeability vs. Reciprocal Mean Pressure at Several Temperatures for Massillon Sandstone Core No. 6, Confining Pressure = 4000 psig	55
23	Apparent Permeability vs. Reciprocal Mean Pressure at Several Temperatures for Ottawa Silica Sand Core No. 16, Confining Pressure = 2000 psig	57
24	Oil Permeability vs. Temperature for Massillon Core So. 10	59
25	Oil Permeability vs. Temperature for Massillon Core No. 11	60
26	2-Octanol Permeability vs. Temperature for Unconsolidated Ottawa Silica Sand Core No. 17	61

1. INTRODUCTION

A long held conclusion that the absolute permeability of a porous medium is a constant determined only by the structure of the medium in question is the subject of this study. Experiments designed to measure the absolute permeability of porous media have shown[1,16] that the absolute permeability to water for certain sandstone cores varies with the level of confining pressure as well as with temperature. For water flow, permeability reductions of up to 60% were observed when temperature was increased from 70°F to 300°F.

This important discovery may have significant ramifications in many oil recovery by thermal processes. The injection of hot water and steam into oil reservoirs, underground combustion, injection of fluids into wells, the production of geothermal energy, and the disposal of atomic waste products in porous formations all cause changes in formation temperatures.

In reservoir engineering, absolute permeability is a basic parameter which has often been measured at room conditions, with the implicit assumption that only confining pressure affected the result. (Of course we ignore the well-known reactions between water and clays.) Hitherto, therefore, a single value of absolute permeability throughout a range of reservoir temperatures has been used in reservoir engineering calculations.

Weinbrandt[16] found for water flow, that the absolute permeability of confined, fired sandstone cores was strongly temperature dependent. Cassé[1] verified the Weinbrandt result. In raising the temperature level of a fired consolidated sandstone core under a confining pressure of 2000 psi from room temperature to 300°F, he observed a reduction in absolute permeability of as much as 65%. With mineral oil flow, or inert gas flow, he found that temperature had no appreciable effect on absolute permeability. Recently, Arihara[2] reported that in his water flow experiments through synthetic cement-consolidated sand cores, he did not observe temperature effects on absolute permeability. However, he applied low confining pressures.

Cassé[1] suggested that clay-water interaction caused the permeability reduction he observed. However, Greenberg, et al. in 1968 reported data on the permeabilities to water of core samples artificially consolidated with phenolic resin or by sintering. The general trend showed slight to moderate decreases in permeability with increasing temperature. No confining pressure was applied to the core. They attributed the observed changes to micro-structural re-arrangements in the matrix geometry of the samples which had a rough and irregular surface. They observed no changes in permeabilities for samples with relatively smooth surfaces.

The purpose of this work was (1) to verify the results of previous studies, (2) to extend the previous work to other systems, and (3) to investigate the reason for temperature

effects on absolute permeability. In order to provide a clue as to what actually caused the permeability to decrease with increasing temperature, it was decided to use clay-free rocks and other polar liquids, such as 2-octanol.

2. FLOW IN POROUS MEDIA

In 1856, as a result of experimental studies on the flow of water through unconsolidated sand filter beds, Henry Darcy formulated a flow law which now bears his name. This law hag been extended to describe, with some limitations, the movement of other fluids, including two or more immiscible fluids, in consolidated rocks and oth r porous media.

2.1 Darcy's' Law

Darcy's law, for the horizontal, viscous flow of a fluid in a linear medium, states that the flow velocity of a homogeneous fluid is proportional to the pressure gradient, and inversely proportional to the fluid viscosity, or:

$$v = -\frac{k}{\mu}\frac{dp}{ds} \qquad (2-\ )$$

where v is the velocity in cm/sec, q is the flow rate in cc/sec, μ is the fluid viscosity in cp, dp/ds is the pressure gradient in atm/cm, taken in the firection of flow, and k is the rock permeability, darcies. A rock of one darcy permeability is one in which a fluid of one centipoise viscosity will move at a velocity of one centimeter per second under a pressure gradient of one atmosphere per centimeter.

Darcy's law applies only in the region of laminar flow. For "turbulent" or non-laminar flows which occur at higher velocities, the pressure gradient increases at a greater rate than does the flow rate.

A correlation produced by Fancher, Lewis, and Barnes[5] may be used to estimate the region of viscous flow for a porous medium. In general, Darcy's law is valid for porous media when a modified Reynolds' number

$$Re = \frac{vd\rho}{\mu} \qquad (2\text{-}2)$$

is less than one. v is velocity, ρ is fluid density, μ is the fluid viscosity, *and* d is the diameter of the average grain size.

A recent study by Geertsma[6] showed that the average grain size should be replaced by a ratio of permeability to porosity to provide a better correlation.

The requirement that the permeability be determined for conditions of viscous flow is best satisfied[7] by obtaining data at several flow rates and graphing flow rate versus pressure drop for liquid and for gas by plotting the product of mean flow rate and pore pressure versus $p_1^2 - p_2^2$ where p_1 is the upstream pressure and p_2 is the downstream pressure. For conditions of viscous flow, the data should plot a straight line, passing through the origin. Turbulence is indicated by curvature of the plotted points.

2.2 Darcy's Law for Gas Flow

In the case of flow of gases, the flow rate is not constant, but increases with the pressure drop, according to Boyle's law. The integrated form of Darcy's law which describes horizontal linear pas flow, under steady state, isothermal conditions is:

$$q = \frac{kAT_a \Delta p p_m}{\mu \bar{z} T p_a L} \qquad (2\text{-}3)$$

2.3 Slip Phenomena in Gas Flow

Kundt and Warburg[8] first showed that a layer of gas next to a solid surface may have a finite velocity with respect to the wall. In case of capillary flow, this would give a greater rate than would be computed from Poiseuille's law. In effect, the gas stream "slips" with respect to the wall. This is not the case for liquid flow. This "slip" phenomena is dependent upon the mean free path of the gas molecules; therefore, gas permeability should be a function of the factors controlling the mean free path. These factors are pressure, temperature, and the nature of the gas itself. When the mean free paths are small, e.g., at high pressures, the permeability to gas should be expected to approach that to liquids. This idea was supported by the Klinkenburg9 study.

Based upon a theoretical analysis of the slip phenomenon in circular capillaries, and assuming an analogous behavior in a porous medium, Klinkenberg[9] developed the relationship between the permeability of a porous medium to gas and to a nonreactive liquid as follows:

$$k_a = k\left(1+\frac{4c\bar{\lambda}}{r}\right) \qquad (2\text{-}4)$$

where k_a is the apparent or observed permeability to gas, k is the absolute permeability to gas at high pressures (presumed equal to the absolute permeability to a single liquid phase), $\bar{\lambda}$ is the mean free path of the gas molecules, r is the radius of a capillary (assumed to be constant), and c is a proportionality factor. The mean free path can be expressed as:

$$\bar{\lambda} = \frac{1}{\sqrt{2}\pi d^2 n} = \frac{RT}{\sqrt{2}\pi p_m N d^2} \qquad (2\text{-}5)$$

where d is a collision diameter, n is the concentration of molecules per unit volume, N is Avogadro's Number, p_m is the mean pressure, T is absolute temperature, and R is the universal gas constant. From Eq. 2-5, Eq. 2-4 becomes:

$$k_a = k\left(1+\frac{4cRT}{\sqrt{2}\pi r N d^2 p_m}\right) = k\left(1+\frac{b}{p_m}\right) \qquad (2\text{-}6)$$

where b is referred to as the Klinkenberg factor, and is usually taken as a constant for a given gas and a given porous medium. From Eq. 2-6, the Klinkenberg factor appears directly proportional to temperature.

2.4 Visco-Inertial Flow

Darcy's law and the preceding equations are valid when conditions of viscous flow prevail. At high flow rates, flow has been shown to be described by a quadratic equation. Such an equation was proposed by Forchheimer[10] and modified by Cornell and Katz[11] as follows:

$$-\frac{dp}{dL} = \mu \frac{v}{k} + \beta \rho v^2 \qquad (2\text{-}7)$$

Dranchuk and Kolada[12] have shown how to delineate the visco-inertial flow region from flow measurements, and how to determine the absolute permeability of a rock core (see Appendix 9.3).

The visco-inertial flow described by Eq. 2-7 is sometimes referred to as "turbulent" flow. The departure from laminar flow described by Eq. 2-7 is not caused by physical factors which cause turbulent flow in pipe. This phenomenon is usually referred to as "non-Darcy," "inertial," or "visco-inertial" flow. We shall use the latter term.

3. LITERATURE

In 1937, Muskat[4] stated that the absolute permeability of a porous medium "is thus a constant determined only by the structure of the medium in question and is entirely independent of the nature of the fluid." Also, the standard prat cedure for determining the permeability of porous medium according to API Code No. 27[15] (first edition, October 1935) was based on the fundamental assumption that as long as the rate of flow was proportional to the pressure gradient, the permeability constant of a porous medium was a property of the medium and was independent of the fluid used in its determination.

A major study by Klinkenberg appeared in 1941. Klinkenberg[9] performed liquid permeability measurements on Jena glass filters in order to avoid clay swelling or erosion. The cores were not confined nor were variations in temperature studied. From his analysis of gas flow through the same cores, he therefore supported the notion that the permeability constant of a porous medium was a property of the medium, and was independent of the fluid used. In addition, he was the first person to explain slip phenomena.

In 1943, Grunberg and Nissan[13] studied the effect of flow of aqueous solutions through limestone and sandstone cores over a range of temperatures. Four solutions were tested:

(1) distilled water, (2) a 2% n-amyl alcohol solution, and (3) two sodium chloride solutions (0.960 and 0.614N). The choice of these solutions was made so as to observe the influence of surface forces on the flow of liquids through porous media. The core temperatures were varied from 6°C to 30°C.

Permeability decreased with increasing temperature for all of the four aqueous solutions. All four gave linear permeability temperature curves with approximately the same slope. The slope of the graphs of permeability vs. temperature was 0.8 md/°C. Thus:

$$k = a - 0.8(t, ^\circ C) \qquad (3\text{-}1)$$

where a is a characteristic constant of the liquid used. As the fluid viscosity was considered properly in calculating permeability, they concluded that viscosity was not the only property influencing flow. In addition, a log-log graph of k/k_1, vs. $\left(\frac{\mu}{\rho\sigma}\right)^2$ gave a straight line. k_1 is a base permeability; μ is fluid viscosity, ρ is fluid density, and σ is surface tension.

A conclusion reached was that the effective cross-section under viscous flow was different for different liquids due to differences in surface energy, and thus differences in the thickness of adsorbed layers.

In 1946, Calhoun and Yuster[14] presented results of flow through artificial porous bodies, some made of pyrex glass and others of fused quartz. No confining pressure was applied.

They disagreed with Grunberg's and Nissan's results and confirmed Klinkenberg's results.

Calhoun and Yuster found that water gave a slightly lower value for permeability than benzene. A suspicion of an electro-kinetic effect was ruled out because addition of a trace of HCl or $CaCl_2$ to the water caused no apparent increase in permeability. Furthermore, naphtha gave a permeability as low as that of water, and, with this hydrocarbon liquid an electro-kinetic effect should have been absent. Calhoun and Yuster were unable to give an explanation of this anomaly. They were the first to observe a dependency of Klinkenberg's factor, b on temperature.

In trying to correlate Klinkenberg b values at different temperatures, Calhoun and Yuster assumed that equal mean free paths would occur at equivalent molecular concentrations at different temperatures, A gas at pressure p_1 and T_1 should have the same molecular concentration as the same gas at a pressure p_2 and T_2, if $\frac{p_1}{T_1}$ were equal to $\frac{p_2}{T_2}$. Therefore, equivalent permeability values should exist for the same gas, when two different temperatures were used, at a mean pressure p_m and temperature T_1, and at mean pressure $p_m(\frac{T_1}{T_2})$ at a temperature of T_2. This correlation at different temperatures was not included in either Klinkenberg's or Grunberg and Nissan's presentation.

In the late 1960s, Greenberg, et al.,[3] and Weinbrandt[16] again observed a permeability dependency on temperature level. Greenberg, et al., did not restrain their cores and observed

only **small** temperature effects. Weinbrandt[16], in his experiments on the effect of temperature on relative and absolute permeability of sandstones, subjected his cores to 2000 psi confining pressure. He also fired the cores at 940°F prior to use to oxidize organic matter in the cores and to deactivate the clays. His experiments for Boise sandstone core samples at room temperature and at 175°F showed that with an increase in temperature: (1) the irreducible water saturation increased; (2) the residual oil saturation decreased; (3) the relative permeability to water at flood-out increased; (4) the relative permeability to oil increased; (5) the relative permeability ratio, k_w/k_o, decreased; and (6) the absolute permeability to water decreased. Cassé[1] verified the Weinbrandt findings and substantially extended the work.

The effect of mechanical stresses on the permeability of rocks has been studied by several investigators. In 1967, Wilhelmi and Somerton[17] investigated the effect of overburden pressure on rock permeability. They confirmed earlier work by Fatt and Davis[18] in 1952, and reported that permeability at 15,000 psi confining pressure could be 25 to 60% smaller than the permeability at a zero confining pressure, depending on the type of rocks studied. Generally speaking, the higher the permeability, the higher the percentage of reduction. About 60% of the total reduction occurred during the first 3000 psi confining pressure.

In 1963, Gray, *et al.*,[19] also measured the effect of overburden pressure on permeability. Permeability reduction was shown to be a function of the ratio of radial to axial

stress, with the maximum reduction occurring under a uniform stress, i.e., when the axial stress is equal to the radial stress. The present work reported here was accompanied under conditions of uniform stress.

Zoback and Byerlee (1975a)[20] showed that due to the presence of compressible matrix material in a relatively incompressible granular framework, the permeability of sandstone is not simply a function of effective stress, but is highly sensitive to changes in pore pressure.

The effect of thermal stresses on rock properties and the effect of overburden pressure on porosity have also been of particular interest.

Somerton, et al.,[21] heated a number of sandstones to about 1500°F under both atmospheric and simulated reservoir pressures. Permeability was measured at room temperature using a standard air perimeameter, before and after heating the samples. No permeability changes were reported in the range of 75-350°F. At temperatures well above 500°F, they showed that permanent structural damage and decomposition of rock minerals occurred due to thermal stresses.

Wyble[22], working on the effect of applied pressure on sandstone's properties, observed asymptotic decreases in conductivity, porosity, and permeability over a 0 psi to 3,500 psi range. At 2000 psi confining pressure, about a 10% reduction in porosity was observed, and beyond this, the porosity value remained essentially constant.

In summary, many studies indicate the likelihood of absolute permeability of rocks being a function of temperature beyond the effects caused by a change in the viscosity of the fluid. The recent works of Weinbrandt[16] and Cassél indicated an effect of major importance for restrained cores. No obvious explanation existed. The main purpose of this study was a verification of and study of possible explanations of these effects.

4. EXPERIMENTAL EQUIPMENT

The experimental equipment used was similar to that described previously by Cassé[1] and Weinbrandt16. Some modifications were made in the apparatus, however. A description of the apparatus follows.

4.1 General Description

Fig. 1 is a photograph of the laboratory, and Fig. 2 presents the details of the air bath assembly. A schematic diagram of the apparatus is shown in Fig. 3. The flow lines, heat exchangers, and fittings were constructed of 316 stainless steel material.

Three parallel flow lines were constructed for gas, oil, water, or 2-octanol injection. For each experiment, the desired flow line was connected to the core; a new core being used for each experiment. Liquid flow was supplied by a pulsating pump, and gas flow was supplied from high pressure cylinders and delivered through precision pressure regulators.

Liquid flow rate through the core was measured by a weighing balance. Depending upon the level of flow rate, gas flow rate was measured either by the use of a bubble film flowmeter or by a Wet Test Meter. A thermocouple was placed at the inlet face of the core, and temperature was recorded continuously during the runs. The core holder assembly was placed in an air bath that maintained run temperature. Measurements of upstream pressure and pressure drop across the

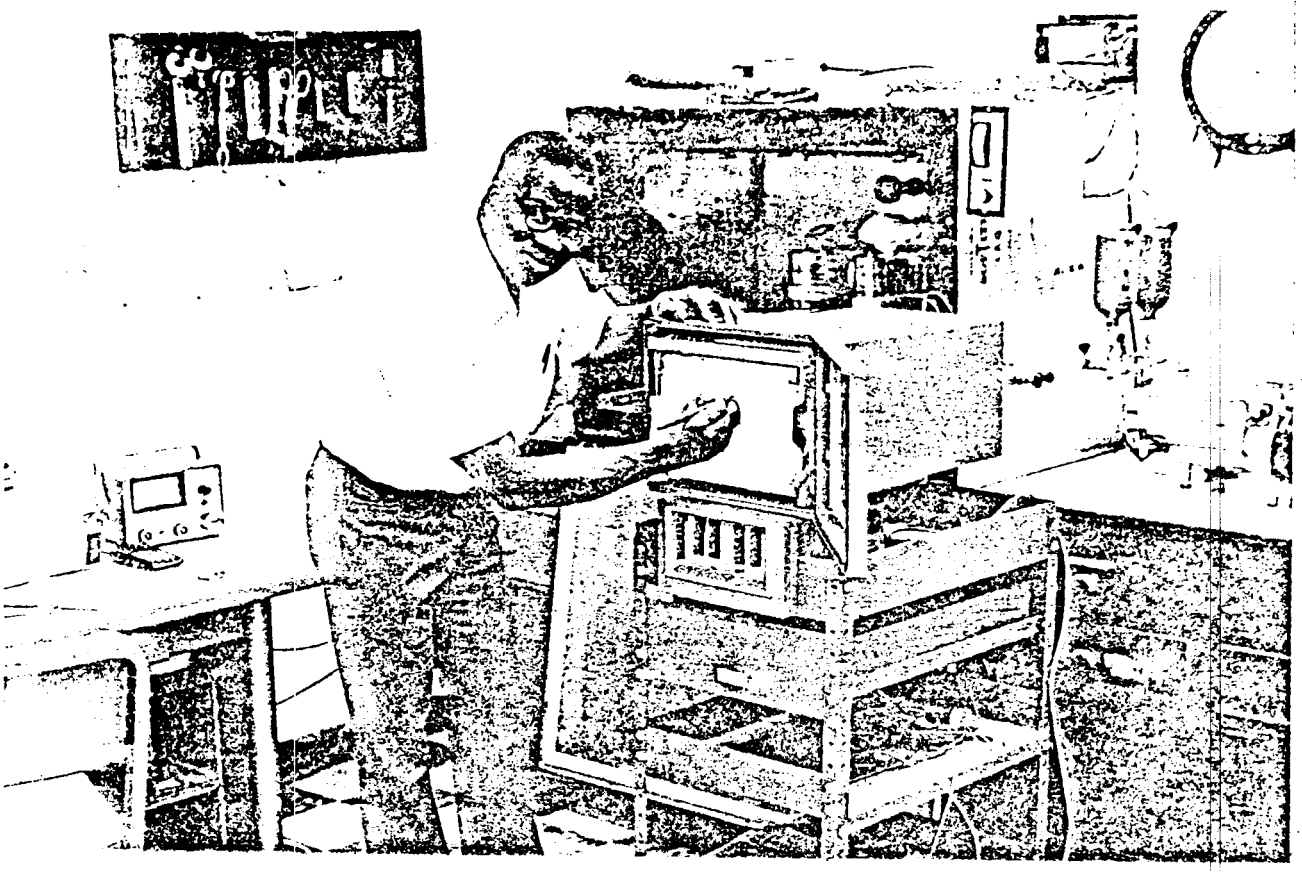

Fig. 1. Photograph of Apparatus

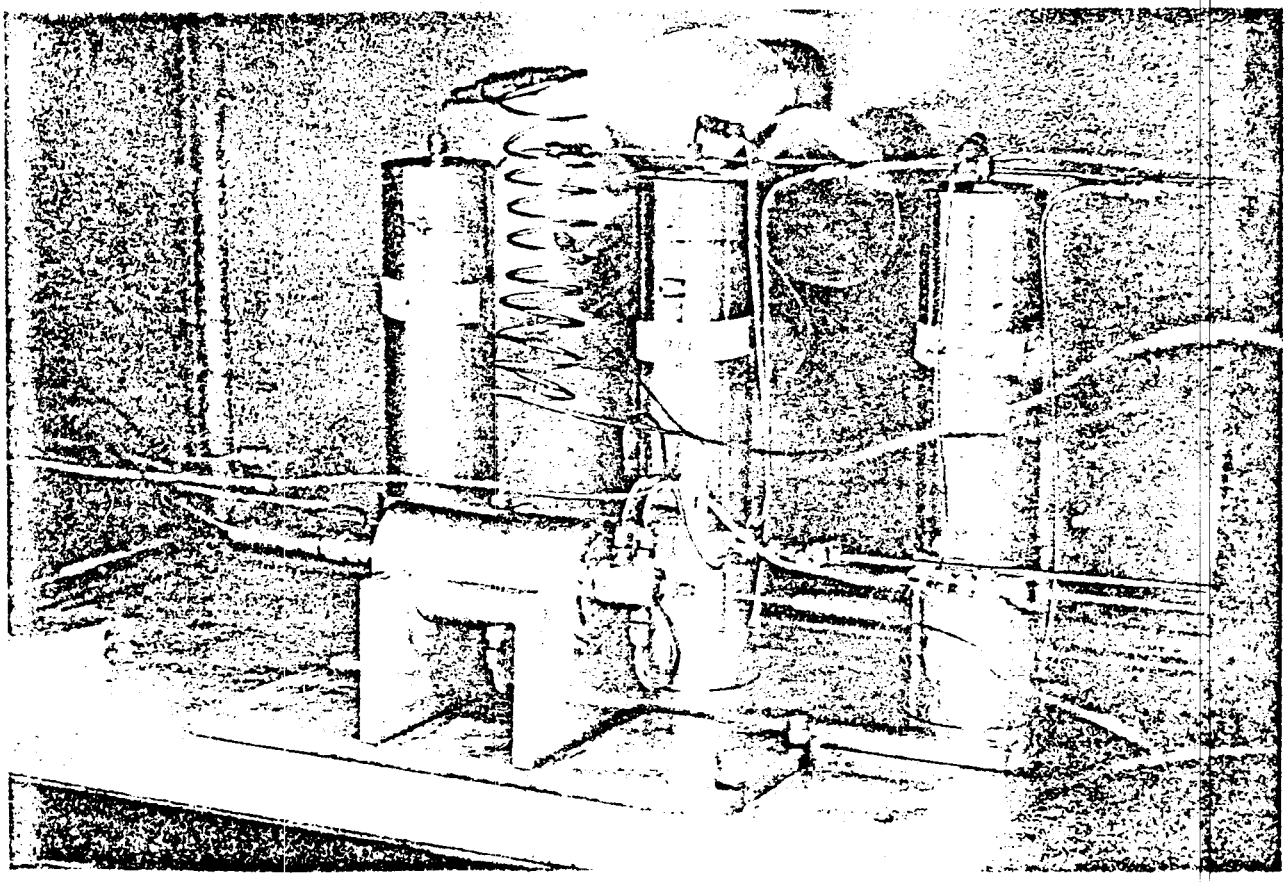

Fig. 2. Details of Assembly in the Air Bath

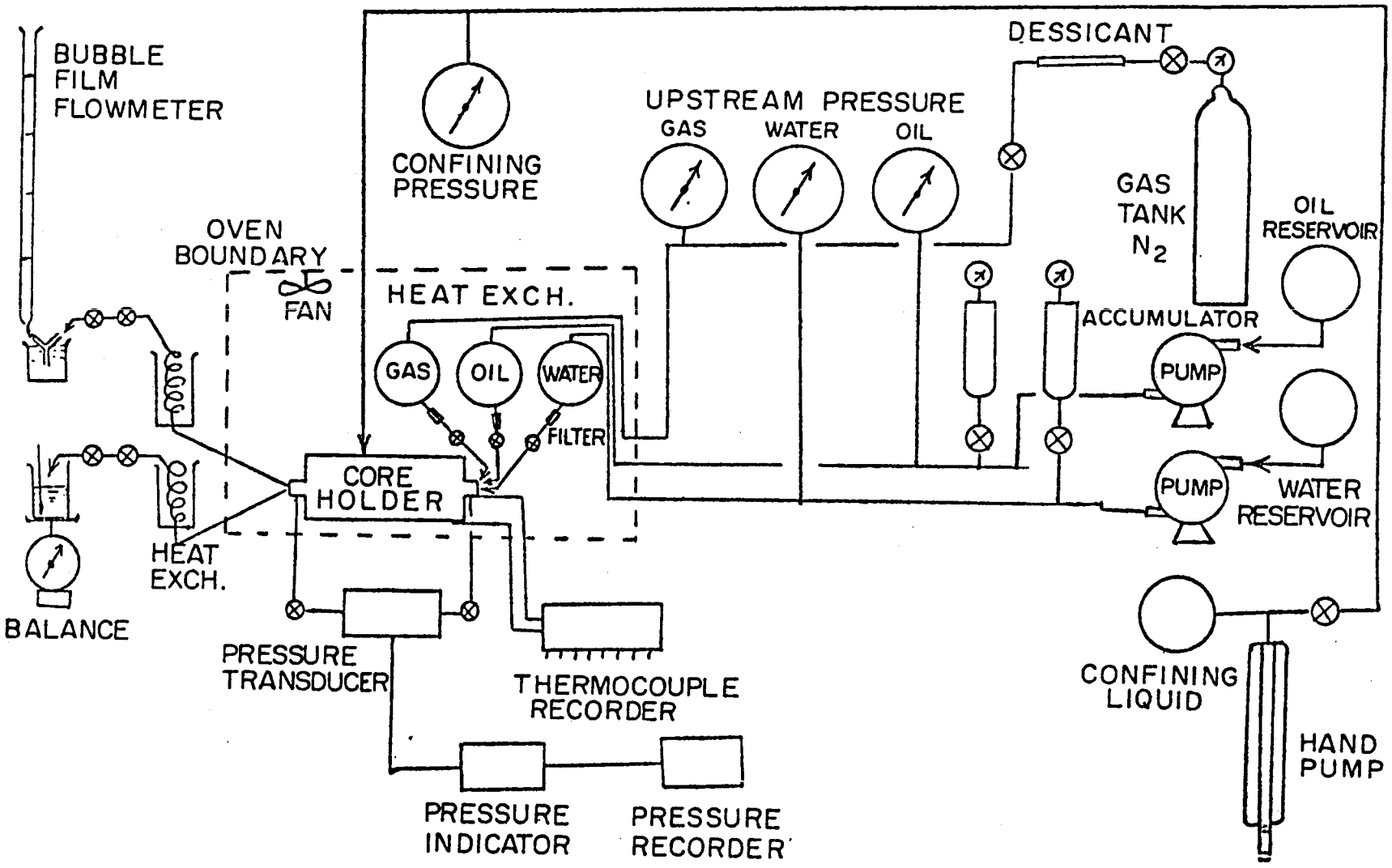

Fig. 3. Schematic Diagram of Apparatus

core were accomplished by the use of pressure transducers connected to pressure indicators and recorders.

The desired confining pressure level was attained by using a hydraulic hand pump. Chevron No. 15 heavy oil was used as a confining fluid and a "Viton A" rubber sleeve, 1/8" thick, separated this fluid from the core.

A description of the major components of the apparatus follows.

4.2 Core Holder

Fig. 4 shows the details of the core holder which is a Hassler rubber sleeve type. The rock specimen to be studied is held in a "Viton A" rubber sleeve, 1/8" thick, between an upstream plug, which is immobile, and a downstrean plug which moves horizontally and adjusts to the core length. The upstream plug has two pressure taps A and D, one tap B for inlet flow:, and a thermocouple well C.

Either liquid or gas pressure can be applied to the Viton sleeve, but throughout these experiments, Chevron White Oil No. 1.5 was used. Both axial and radial confining pressures are applied simultaneously to the core because the downstream plug, is mobile and subject to the confining pressure. A perforated aluminum tube is fitted around the core rubber sleeve to prevent lateral deformation of core during loading. The sleeve was a thick cylinder 1.225 in. ID by 1.946 in. OD by 3.0 in. long.

4.3 Air Bath and Temperature Control

An air bath with a working space of 24 cubic feet housed the core holder assembly. Four kilowatts of power may

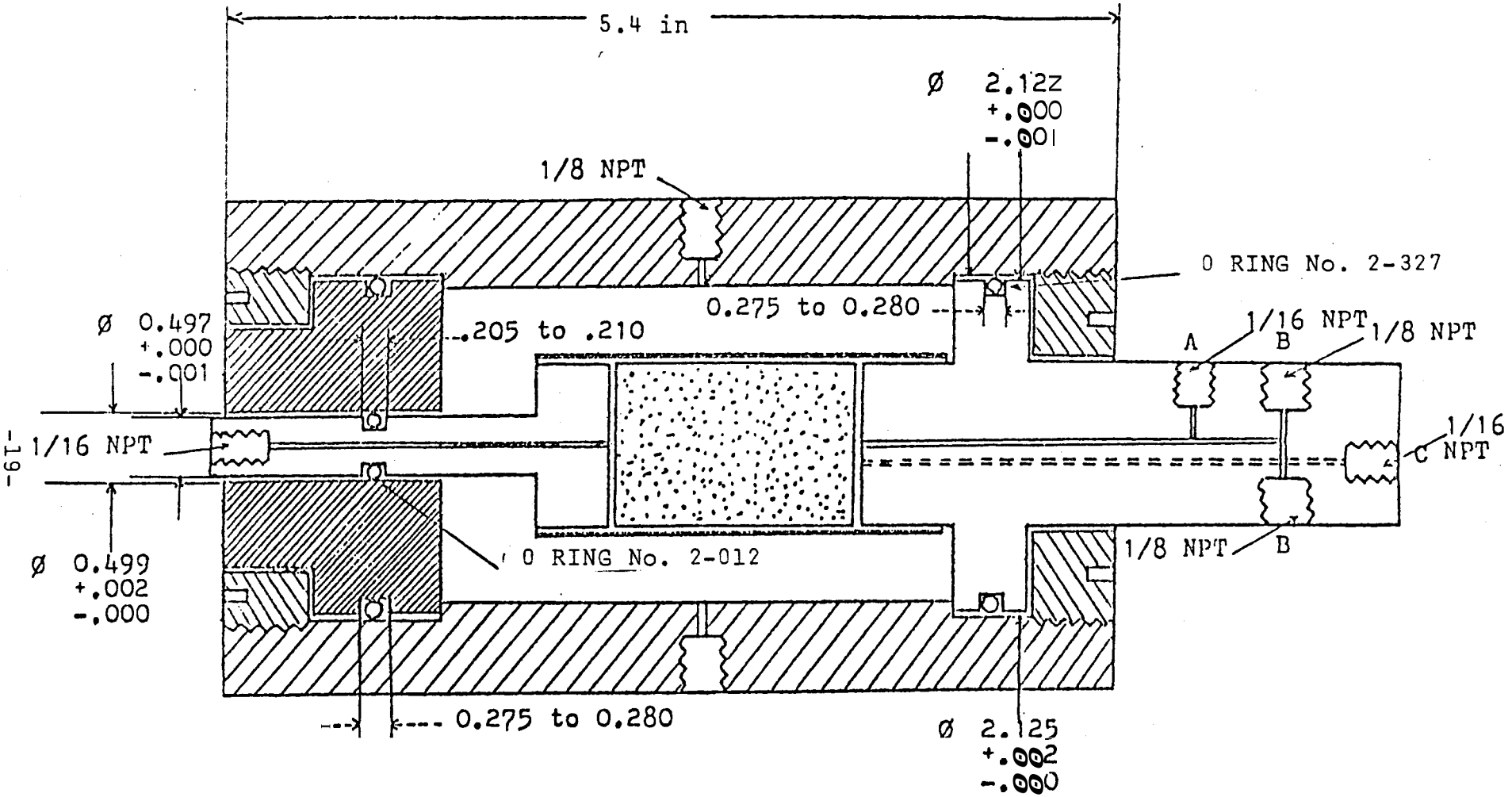

Fig. 4. Schematic Diagram of the Core Holder

be applied to the heating elements by an API model 4010 power pack and an API model. 228 temperature controller. The thermocouple that controls the output of the heater controller can be placed at any location inside the oven, but the most efficient heating cycle was found to result when the thermocouple sensor was fastened tightly to the core holder. A fan provided adequate air circulation and the air bath was equipped with a light and a window.

Temperature was monitored by a 24-point thermocouple recorder with iron-constantan thermocouples. Two thermocouples were actually used. One thermocouple measured the temperature of the core, and the other measured the air bath temperature. The air bath temperature reached the desired test temperature in about 1-1/2 hours, but at least another four hours were required for the rock specimen to reach the test temperature.

4.4 Liquid and Gas Sources

A deaerated liquid was stored in a 4000 cc capacity vacuum flask. A Lapp "Microflo" Pulsafeeder pump was used to pump the liquid through the core. The pump has a dial indicator, calibrated in 1000 increments which enabled fine adjustments in flow rate to be made. Three types of liquids were used: water, oil, and 2-octanol.

Gas flow through the samples was supplied from high pressure cylinders, and regulated by a two-stage adjustable regulator equipped with a relief valve. The initial cylinder pressure was 2500 psi, and delivery pressures ranged from 5 psi to a maximum of 400 psi.

4.5 Liquid Pumps

The pumps were a Lapp "Microflo" Pulsafeeder type with a dial indicator calibrated in 1000 increments. Both pumps created large pressure pulsations when delivering at high pressures. Accumulators, inserted along the flow lines, eliminated these pulsations. A steady flow could be established and constant pressures maintained at both ends of the core.

4.6 Hydraulic Hand Pump

An Enerpac hydraulic hand pump with a range of 0 to 10,000 psi provided adjustment of the confining pressure. The pump was connected to the core holder and Chevron White Mineral Oil No, 15 was used to obtain the desired confining pressure.

4.7 Heat Exchangers

To maintain the temperature of the flowing fluid constant during a run, large reservoirs were installed on each flow line inside the oven before the core holder. Cold fluid entered at the bottom of the reservoir. Because of the large size of the reservoir and the small flow rates that were used with liquid flow, hot fluid left from the top. The temperature of the liquids leaving the reservoir and entering the core was measured and found to remain constant at the desired test temperature during the entire run.

The gas reservoir inside the oven was filled with stainless steel wool. This improved heat exchange and enabled the gas to reach the test temperature before entering the core.

The effluent from the core and the air bath was cooled prior to flow rate determination. This was accomplished by letting the effluent flow through a coil immersed in a constant room temperature water bath.

4.8 Backpressure Valve

Backpressure was regulated by means of a fine metering needle valve. This valve, in addition to being used to change the flow rate, served to maintain a sufficiently high pressure in the system to keep the operating liquid in the liquid state. By adjusting the valve and the pump rate, a constant mean pore pressure could be maintained. Maintaining a constant mean pore pressure level was important because experimental work by Zoback[20] showed that a change in mean pore pressure could affect absolute permeability to an even greater extent than did a change in confining pressure. A constant mean pore pressure of 200 psi was maintained for all liquid runs.

4.9 Flow Rate Measuring Devices

4.9-1 Liquid Flow: At steady state, the mass flow rate was constant throughout the system. The mass flow rate was measured by weighing small volumes of the effluent liquid by an analytical balance over a known period of time. Repeated measurement permitted checking determination of steady state. The volumetric flow rate within the core was determined as the ratio of the mass flow rate to the density of the liquid at run temperature and mean pressure. The flow rate could

be changed by adjusting the pump rate and/or by adjusting the needle valve.

4.9-2 Gas Flow: Gas pressure was regulated upstream by a two-stage pressure regulator and gas flow was regulated downstream by means of a needle valve. The choice of the appropriate flowmeter was made according to the level of flow, i.e., laminar flow (low rate), or visco-inertial flow (high rate). A bubble film flowmeter was used for all laminar flow measurements and a Wet Test Meter was used for visco-inertial flow measurements. A stop watch, graduated in divisions of 0.2 second, was used as a timing device.

The bubble film flowmeter was the most accurate of the two devices, and was used to check the Wet Test Meter at low flow rates. The bubble film flowmeter was made as follows. The vertical part of a Y-shaped tube is plunged just up to the throat in a soap solution (see Fig. 1). The gas flow to be metered enters through one of the branches and bubbles into the other branch arid then up into the vertical burette. The flow rate is obtained by measuring the time it takes for a bubble to traverse a known volume in the burette. This method essentially provided flow rate measurements at room conditions because the pressure required to displace the bubbles was always less than 0.01 psi.

4.10 Pressure Recording Devices

Upstream pressure and pressure drop across the core were measured with a Pace Model KP15 differential pressure

transducer and a Pace Model CD25 transducer indicator. The appropriate plate (1 psi, 5 psi, 25 psi, 100 psi, or 500 psi) was used for the working range of pressure or pressure drop. An electronic two-pen multi-range recorder, "Chessell," was connected to the indicator and provided a permanent record of the pressure. A Barnett Dead Weight Tester was used to calibrate the pressure recording devices.

5. PROCEDURE

Core samples to be studied were held, completely saturated with the desired liquid, in a Hassler, rubber sleeve type core holder, in an air bath. The temperature of the air bath and that of the core were then brought to the desired level. Flow was established, and after reaching a steady-state condition, the necessary pressure measurements and flow rates were measured. With the necessary corrections for the effect of temperature on fluid viscosity and density, absolute permeability of the core was computed at run temperature The liquids used were water, Chevron White Oil No. 3, and 2-octanol. Nitrogen was the gas used.

5.1 Core Preparation

The two types of 'rocks used in this study were consolidated Massillon Sandstones, and unconsolidated Ottawa Silica Sand. With the exception of the first run with each type, i.e., experiments No. 2 and No. 14, the cores were fired for at least 12 hours in a 500°C furnace so as to oxidize any organic matter present.

5.1-1 Consolidated Massillon Sandstones: The cores were cut with a one-inch diameter diamond drill, trimmed on a lathe, extracted in a Dean Stark type apparatus, and ignited in a 500°C furnace. Full details of the process are given in Ref. 1.

After ignition, the cores were saturated under vacuum with the desired flowing liquid. The difference in weight at 100% liquid saturation and a totally dry condition was used to calculate the core porosity.

For nitrogen flow, the air-saturated core was mounted in the core holder and flushed with several pore volumes of nitrogen.

Details of the physical and mineralogical properties of these cores appear in Appendix 9.2.

5.1-2 Unconsolidated Ottawa Sand: The sand was sieved and separated into uniformly graded sizes. For one run, experiment No. 14, the sand that passed through sieve No. 35 but retained in sieve No. 45 was used. For all the other runs, the sand size that passed through sieve No. 80 but was retained in sieve No. 100 was used. This gives average sand grain sizes of 0.385 mm and 0.156 mm respectively. The sand was ignited at 500°C.

The core loading and assembly programwas as follows: The upstream plug was inserted into the rubber sleeve and tightly tied to it with 20 gage stainless steel wire. With the assembly held vertically upright, a No. 400 stainless steel mesh, one inch in diameter, was seated on the upstream plug, and the sand was poured into the sleeve slowly. When the sand was about 2 inches high in the sleeve, another similar mesh was placed on top of sand pack and the downstream plug was introduced and also fastened in the same manner. The assembly was then placed in the core holder and

again well compacted and tightened with the help of a vice. The final overall measurement of the core holder was used to calculate the actual length of the core in place. The diameter of the core was the same as that of the end plugs (1-inch diameter).

With the core holder placed in the air bath and connected to the flow line, the core and the flow line were completely evacuated and, while under vacuum, flow was started so as to completely saturate the core and fill the lines with the liquid.

The details of the physical and mineralogical properties of these cores also appear in Appendix 9.2.

5.2 Establishing Run Conditions

With the core in the core holder, the entire assembly was placed in a cradle in the air bath and all necessary connections were made to the flow lines, pressure taps, and core temperature probe.

Confining pressure was then applied slowly by pumping Chevron White Oil No. 15 around the core sleeve, care being taken to displace all the air in this line by opening the core end of the line during the initial stage of pumping. A decreasing confining pressure with time usually indicated leakage of the confining fluid into the core and flow system. To avoid leakage, a 20 gage stainless steel wire was always tied around the rubber sleeve between the end plugs and the rock before assembly.

Air that might have been trapped in the core and the flow system was removed by connecting a vacuum pump to

the outflow end of the system, and applying vacuum for at least five hours. Before the vacuum pump was disconnected, flow was started so that the whole system was completely filled with the liquid to be used.

The assembled system was then heated to the desired run temperature after taking room condition measurements. The air bath temperature reached the desired test temperature in about 1-1/2 hours, but at least another four hours were required for the rock specimen to reach the test temperature. During temperature changes, the confining fluid underwent thermal expansion or contraction depending upon whether heating or cooling. Repeated manual adjustments were made to keep the overburden pressure within the desired level.

When equilibrium temperature was reached, fluid flow was started and continued for about an hour before measurements were taken.

Repeated measurements of temperature, pressures, and flow rate were made at regular time intervals. Steady state was assumed when no change was observed in the readings and the steady values were recorded. All flow rate measurements were taken at room conditions.

5.3 Measurements and Calculations

5.3-1 Liquid Flow: Three kinds of liquids were used in this work: distilled water, mineral oil, and alcohol.

Tap water was distilled in a Barnstead stainless steel still. The oil used was Chevron White Mineral Oil No. 3, and was commercially available. The physical properties of

the oil varied slightly from one container to another. The alcohol used was 2-octanol (Practical). Before use, each liquid was deaerated under a vacuum of about 0.3 psia and filtered.

To keep the fluid in the liquid state at high temperatures, the exit flowing pressure was kept constant at 200 psi for all runs. An accumulator, charged to 200 psi, helped dampen pump pressure pulsations and also helped to keep the flowing pressure from changing drastically when the flow was started or stopped.

Darcy's law for viscous flow in a horizontal and linear porous medium is:

$$q = - \frac{kAdp}{\mu ds} \qquad (5-1)$$

where q is in cc/sec, k is in darcies, μ in cp, A is in cm2, and $\frac{d}{-}$ in atm/cm.

Eq. 5-1 can be expressed as:

$$k = -14700 \frac{L\mu w}{\Delta p A \rho} \qquad (5-2)$$

where k is in md, Ap is in psi, w in gm/sec, ρ in gm/cc, and the other units and symbols are as defined previously. This equation was used in all calculations.

In addition to using Refs. 5 and 6 to estimate the region of viscous flow where possible, conditions of viscous flow were also determined by obtaining data at several flow rates at each temperature level and graphing flow rate, q,

versus pressure drop, p. For conditions of viscous flow, the data should fall on a straight line, passing through the origin. The onset of non-Darcy flow was indicated by a downward curvature of the plotted points from the straight line.

It is necessary to know the viscosity and density of each liquid at each working temperature level. Water density and viscosity versus temperature were found in the Steam Tables[23] and are presented in Figs. 5 and 6, and in Table 1, Appendix 9.1.

A capillary tube viscometer was constructed to measure oil and alcohol (2-octanol) viscosities versus temperature at the working pressure level of 200 psi. The procedure for these measurements is presented in detail in Appendix 9.3. The results of these measurements checked very closely with the data supplied by the manufacturers and those found in Ref. 39. The density of alcohol at various temperatures was measured with a Bingham type pycnometer. The density of the oil was measured at 60°F and the tables in Ref. 24 were used to estimate the densities at higher temperatures. Results are shown in Figs. 7 through 10, and Tables 3 through 5 in Appendix 9.1.

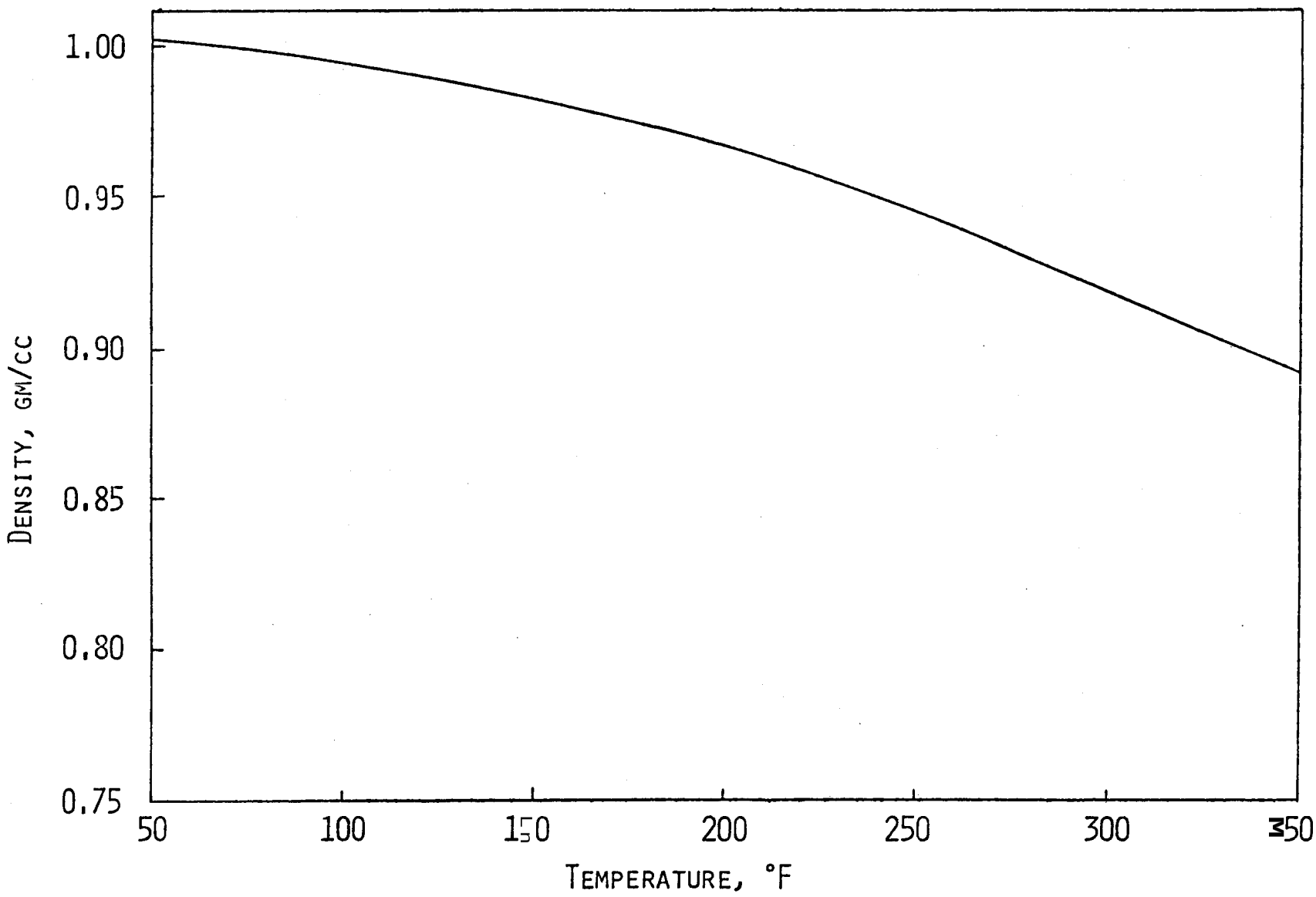

Fig. 5. Density of Water vs. Temperature at 200 psig

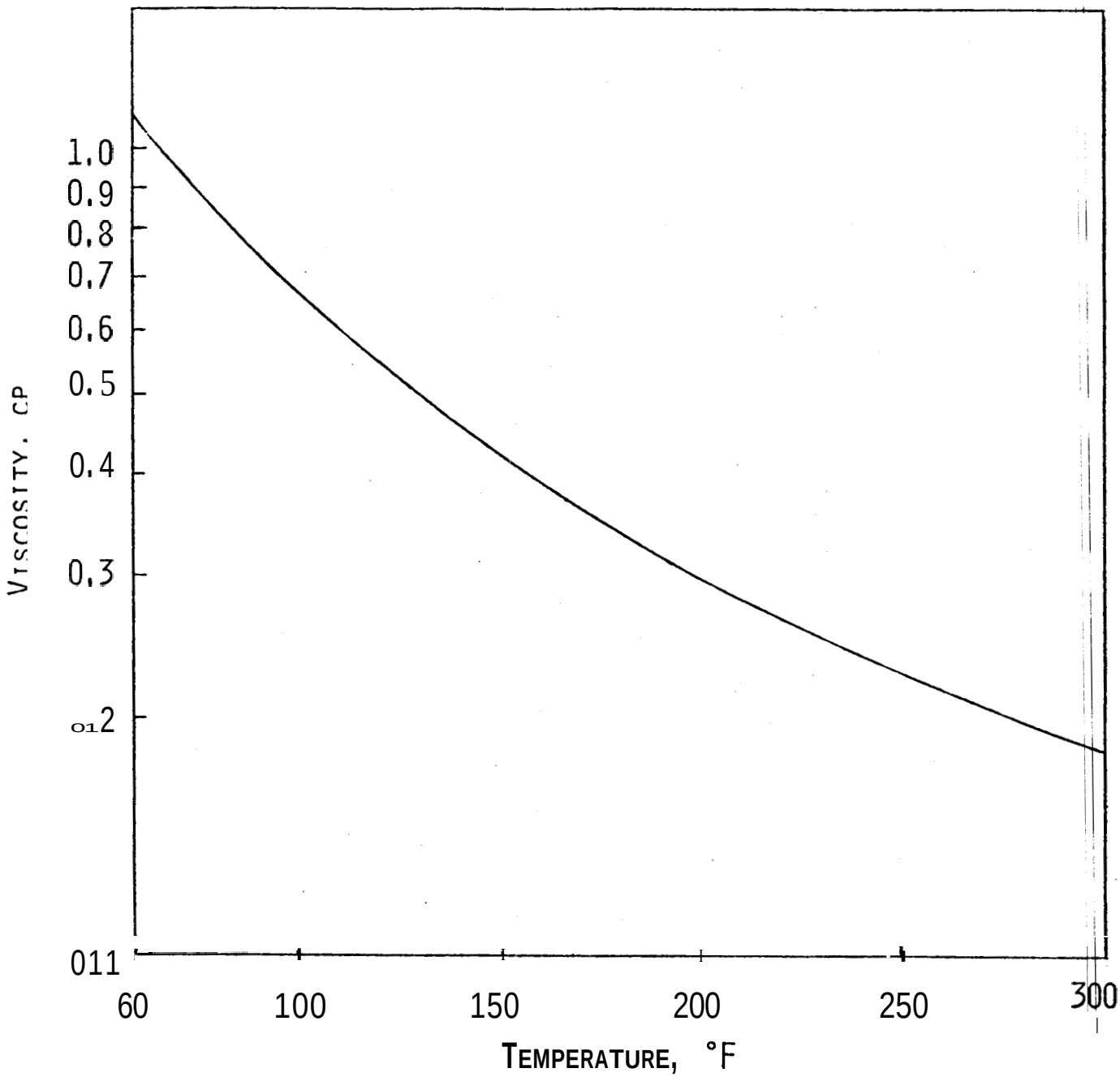

Fig. 6. Water Viscosity vs. Temperature at 200 psig

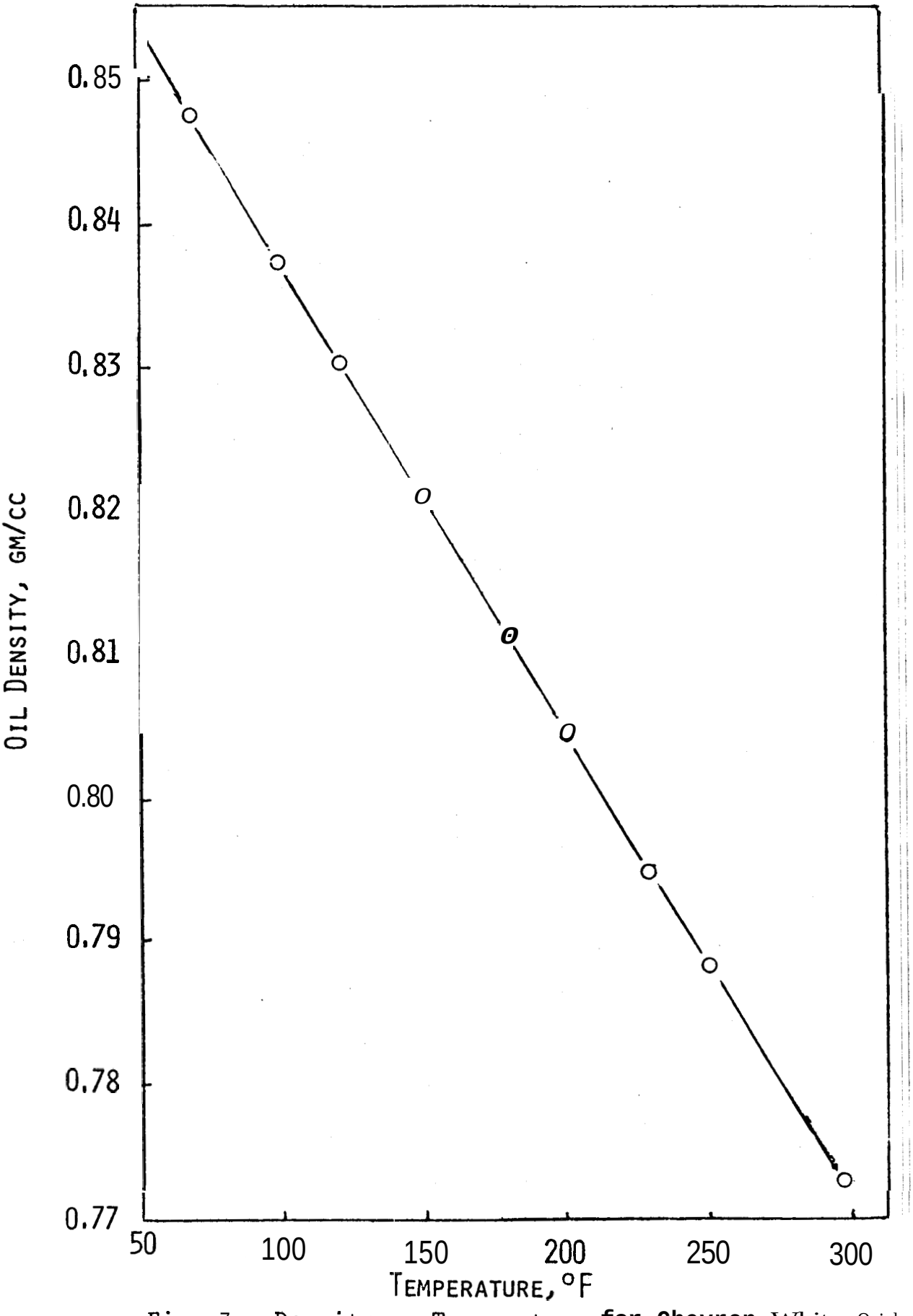

Fig. 7. Density vs. Temperature for Chevron White Oil No. 3

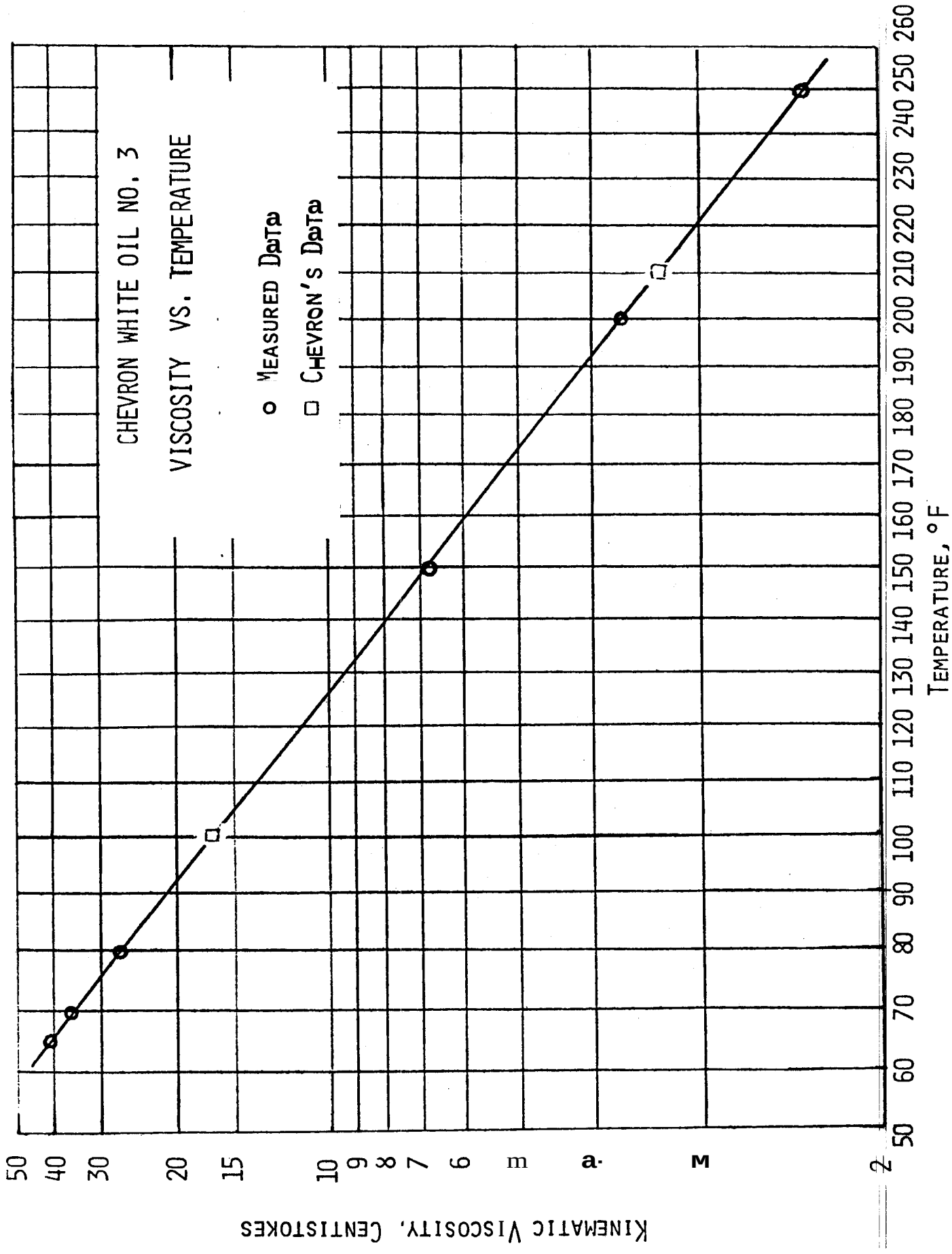

Fig. 8. **Viscosity vs.** Temperature **for** Chevron White Oil No. 3

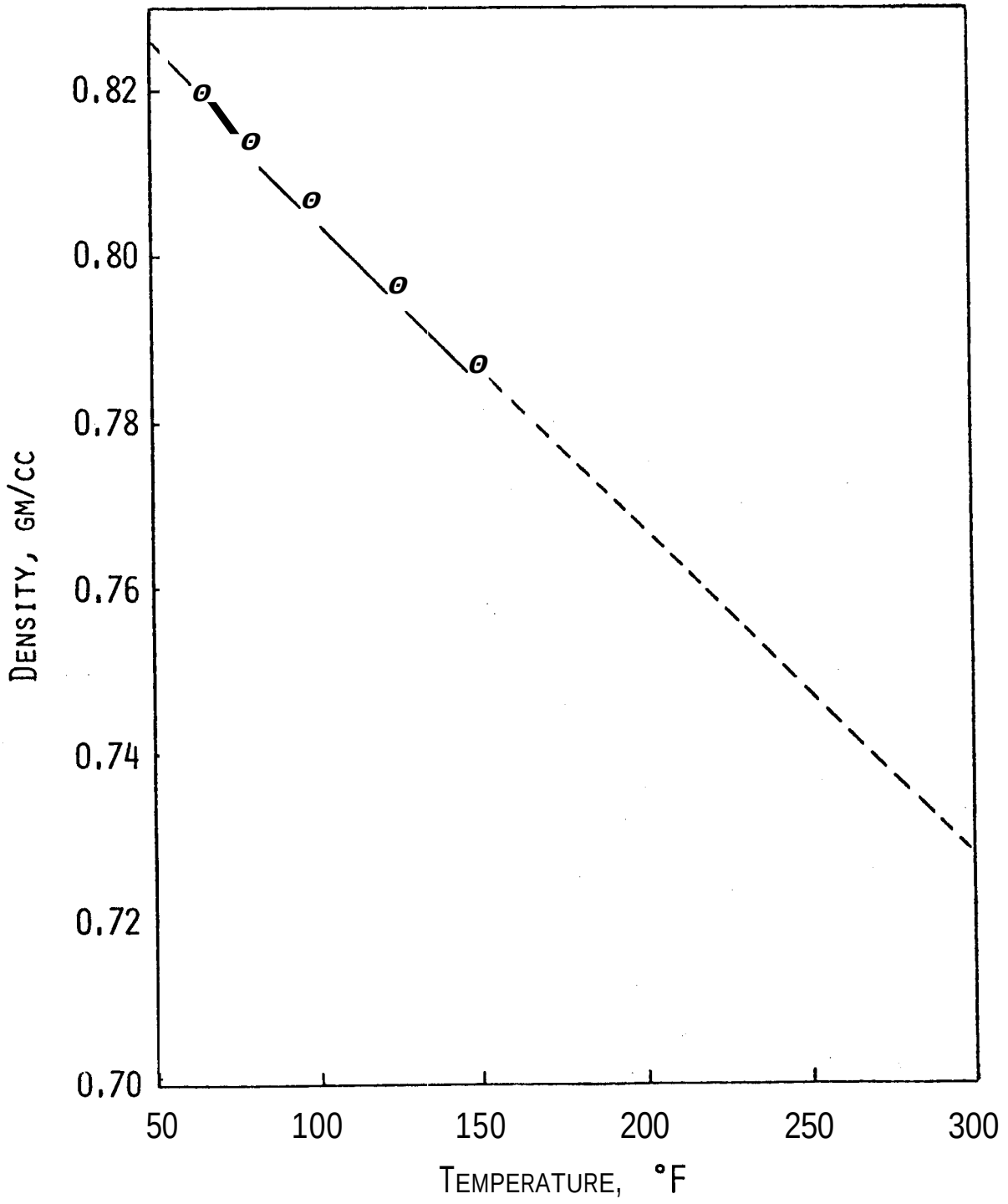

Fig. 9. Density of 2-Octanol vs. Temperature at 14.7 psi.

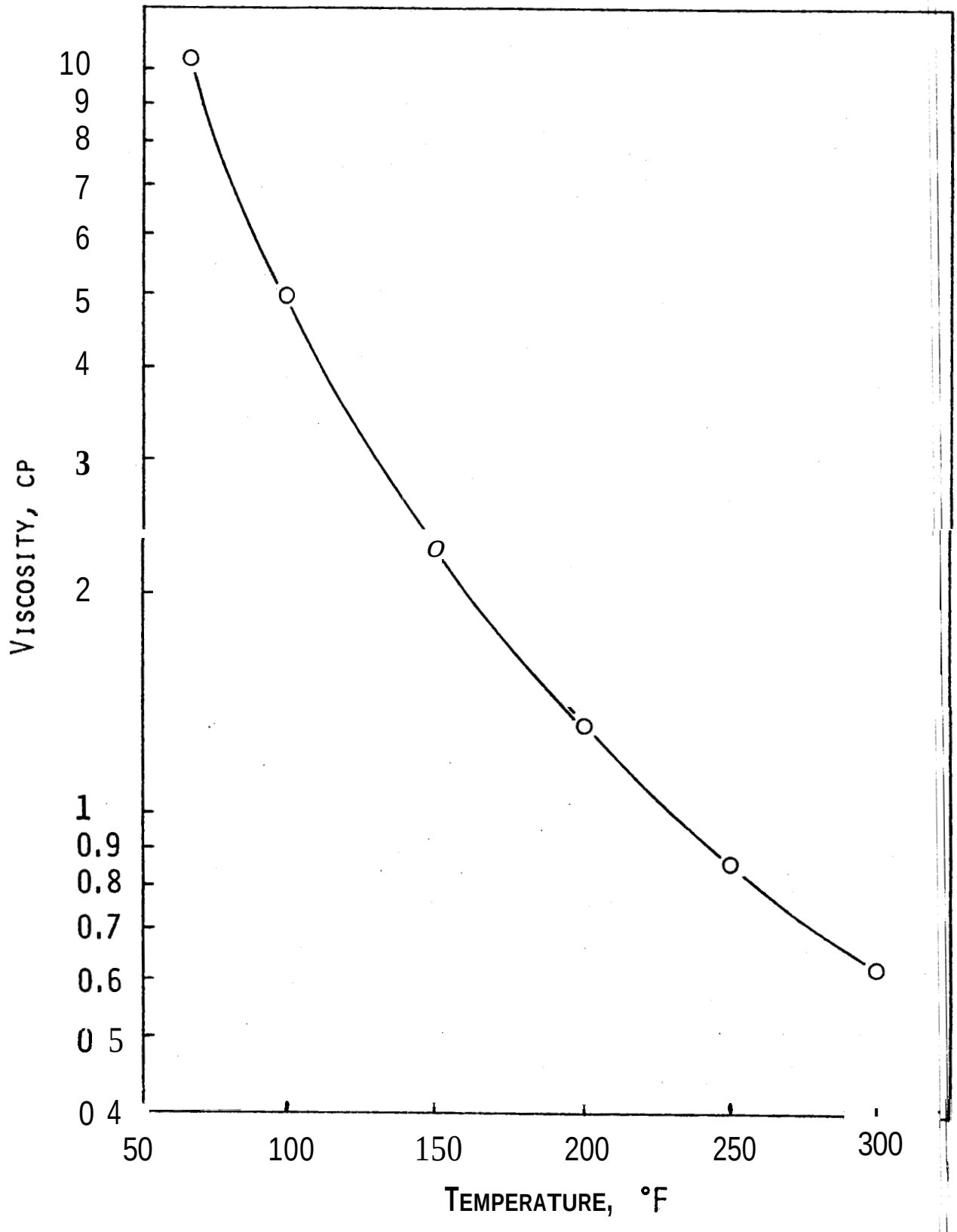

Fig. 10. Viscosity of 2-Octanol vs. Temperature at 14.7 psi

5.3-2 Gas **Flow**: Gas was supplied from high pressure cylinders, and flow rate could be regulated upstream of the core by a two-stage adjustable regulator equipped with a relief valve, and downstream by means of a needle valve. **Most** experiments involved laminar flow in order to obtain absolute permeability and the Klinkenberg slip factor. One visco-inertial run was made.

In addition to measuring pressure drop, Ap, a separate transducer was used to measure the upstream pressure, p_1. From these values, the mean pressure $p_m = p_1 - \frac{\Delta p}{2}$ was computed, **and** the difference $(p_1^2 - p_2^2)$ was calculated as $2p_m\Delta p$.

Low **flow** rates were measured with a bubble film type flowmeter and a Wet Test Meter was used for high **flow** rate measurements. Atmospheric pressure and **room** temperature were also recorded to permit corrections to flowing conditions.

The integrated form of Darcy's law which described steady horizontal linear gas **flow** under isothermal condition$ is:

$$q_a = \frac{kAT_a\Delta pp_m}{\mu\bar{z}Tp_aL} \qquad (5-3)$$

where:

q_a = gas flow rate at room conditions, cc/sec

k = absolute permeability, darcies

A = cross sectional area of porous medium, cm^2

L = length of porous medium, cm

T_a = room temperature, ^oK

T = flowing temperature, ^{o}K

p_a = room pressure, atm. abs.

Δp = pressure drop across porous medium, atm.

p_m = mean pressure within porous medium, atm. abs.

μ = gas viscosity at T and p_m, cp

$\bar{z}$ = mean gas compressibility factor

Nitrogen was treated as an ideal gas and $\bar{z}$ taken as 1 because of the low working pressure range. The right hand side of Eq. 5-3 was divided by 14,700 because, in the laboratory, pressures were measured in psi and permeabilities calculated in millidarcies. Thus:

$$k, \text{ md} = 14{,}700 \frac{L\mu q_a P_a T}{A\Delta p p_m T_a} \qquad (5\text{-}4)$$

Gas viscosity versus temperature is given by Sutherland's formula[25].

$$\mu = \frac{AxT^{1.5}}{B+T} \qquad (5\text{-}5)$$

For nitrogen, N_2:

$$\mu_{N_2} = \frac{13{,}85(10^{-4})T^{1.5}}{102+T} \qquad (5\text{-}6$$

where T is in oK and μ is in cp. Nitrogen viscosity versus temperature at atmospheric pressure is presented on Fig. 11 and in Table 2, Appendix 9.1. No significant increase in nitrogen viscosity occurs from atmospheric pressure to the operating levels, 200 psi., used in this study.

Eqs. 5-4 and 5-6 were used in gas flow calculations for viscous flow. See Appendices, section 9.3-2, for analysis

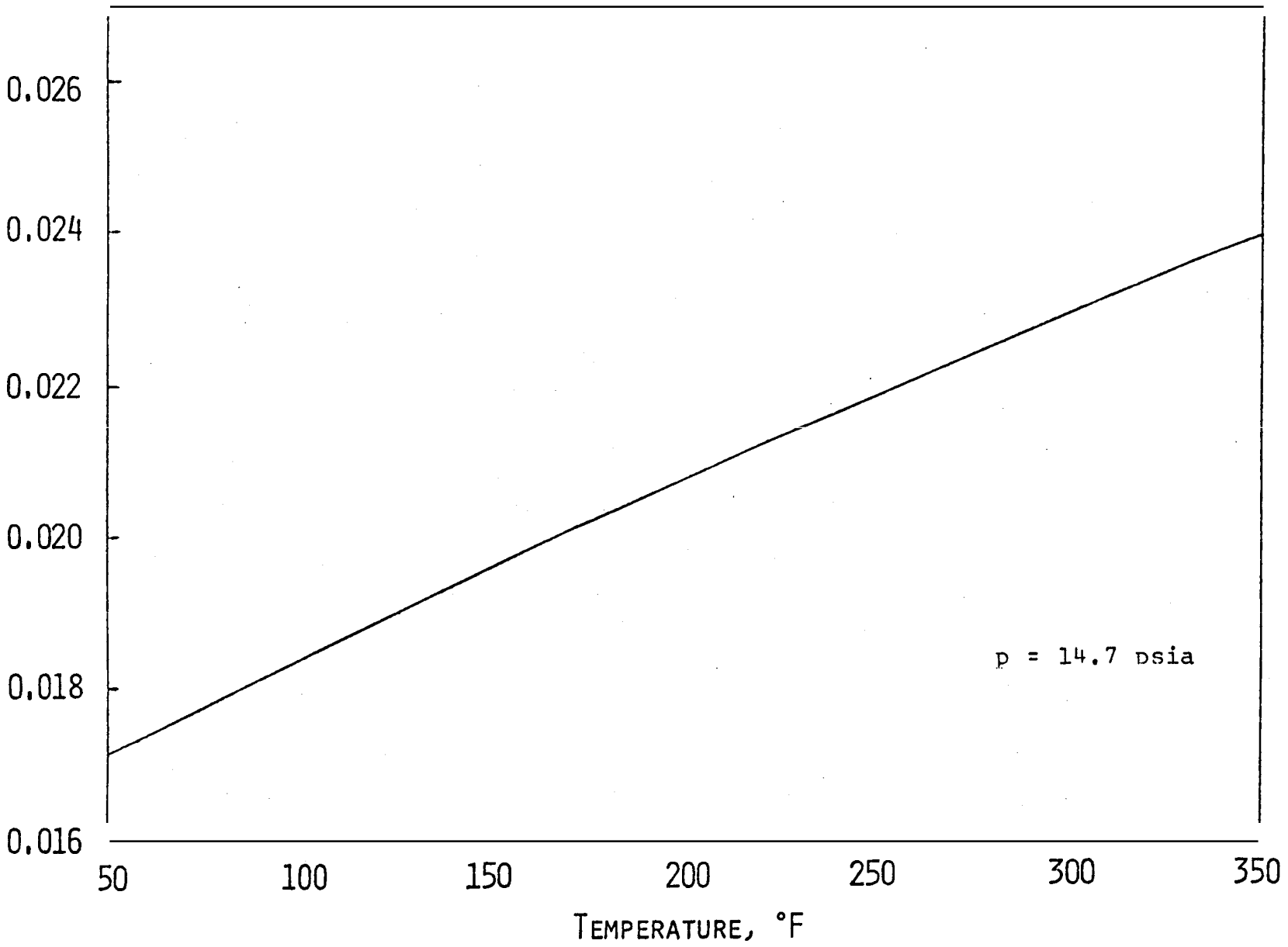

Fig. 11. Viscosity of Nitrogen vs. Temperature

of visco-inertial flow. A linear graph of $(p_1^2-p_2^2)$, (psia)2, where p_1 is upstream pressure (psia), p_2 is downstream pressure (psia), versus gas flow rate, g, (cc/sec), was used to determine conditions for viscous flow.

6. ANALYSIS OF RESULTS AND DISCUSSION

The following presents the results found for the effect of temperature level and confining pressure on single-phase flow in sandstones. Confining pressure had the effect of reducing the absolute permeability of sandstones for all types of fluids used. Slip factor for gas flow was found to be temperature dependent as predicted by theory. A change (decrease) in absolute permeability with temperature increases was observed only in the case of water flow.

6.1 Water Flow

Both consolidated and unconsolidated sandstones were used in this study.

6.1-1 Consolidated Sandstones: The first experiment was carried out with a core that was heated to 300°C for 3 hrs and allowed to cool overnight before use. Fig. 12 presents the result. The rock was first held at 1000 psi confining pressure, and the absolute permeability was recorded with temperature increasing to 300°F. The rock was then allowed to cool to room temperature. Confining pressure was increased to 2000 psi and the process of heating and measurement repeated. The core holder used in the work reported herein is rated at 5000 psi at 350°F safely, but a maximum of 4000 psi and 300°F was used.

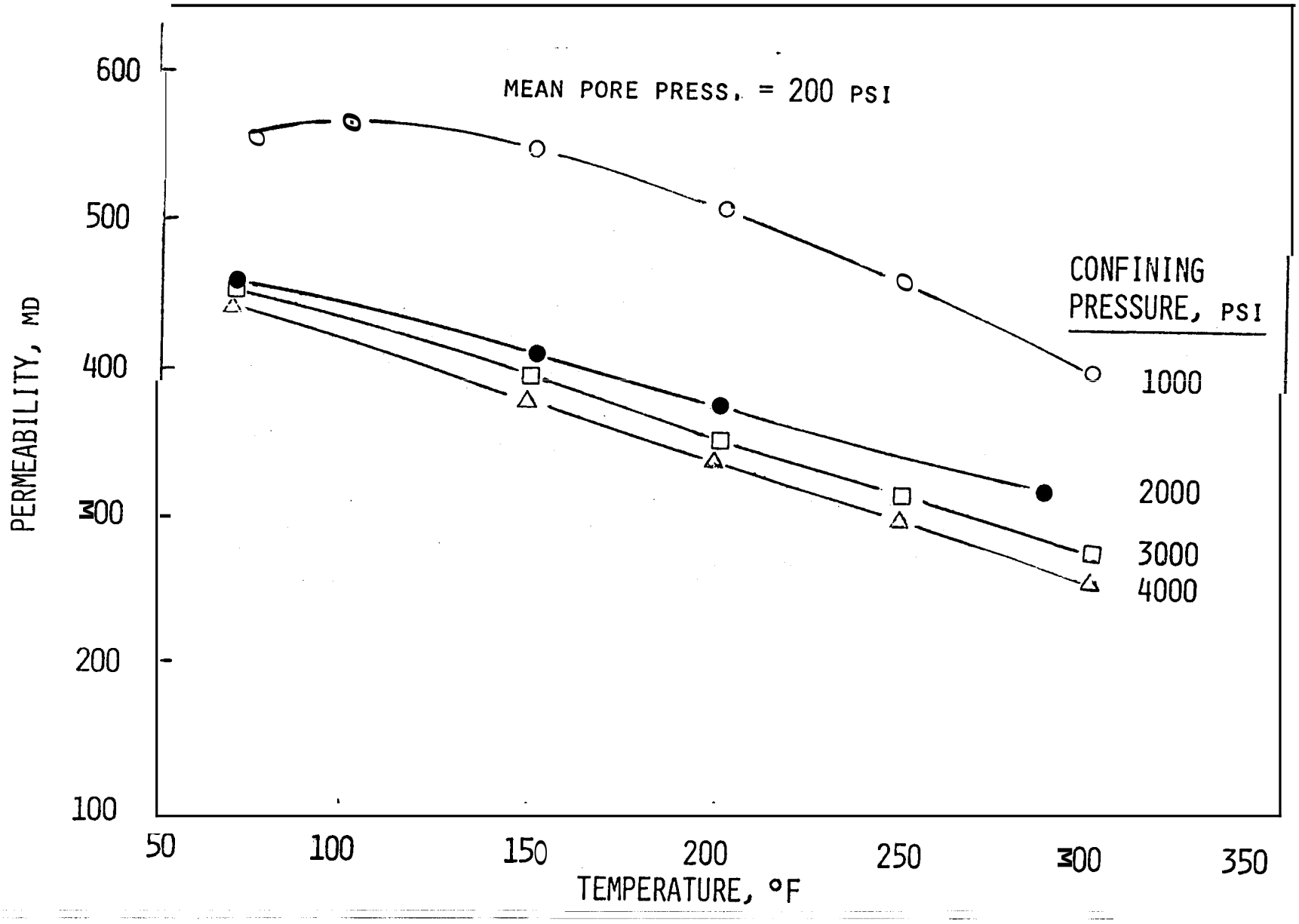

Fig. 12. Water Permeability vs. Temperature, Massillon Sandstone Core No. 2

It can be seen from the graph that at each level of confining pressure, the absolute permeability to water decreased at an approximate rate of -1.0 md/°F.

The next series of experiments were performed on cores fired at 500°C in order to investigate hysteresis and reproducibility of results. The results are shown on Figs. 13, 14, and 15. All showed a decrease of absolute permeability to water with temperature increase, but the slope decreased with increasing temperature. An average slope of -1.3 md/°F to -1.6 md/°F was observed. The results also show that the temperature effect was essentially reversible (see Fig. 13).

The first cooling cycle for the Massillon Sandstone No. 3 (Fig. 14) at 3000 psig confining pressure indicated hysteresis. On the first cooling cycle, the permeability increased with respect to the first heating cycle. On heating and cooling again, results followed the first cooling run, indicating temperature reversibility arid good reproducibility. No reason for the increase in permeability after the first heating run was found.

6.1-2 Unconsolidated Sand: The first experiment in this series was run with unconsolidated Ottawa Silica Sand of average grain size of 0.385 mm. This core was not subjected to heat treatment and was loaded as outlined in the procedure, section 5. Data were not: obtained for the cooling cycles. The results are shown in Fig. 16. Confining pressures of 500, 1000, and **1500** psig were used. Absolute permeability to water

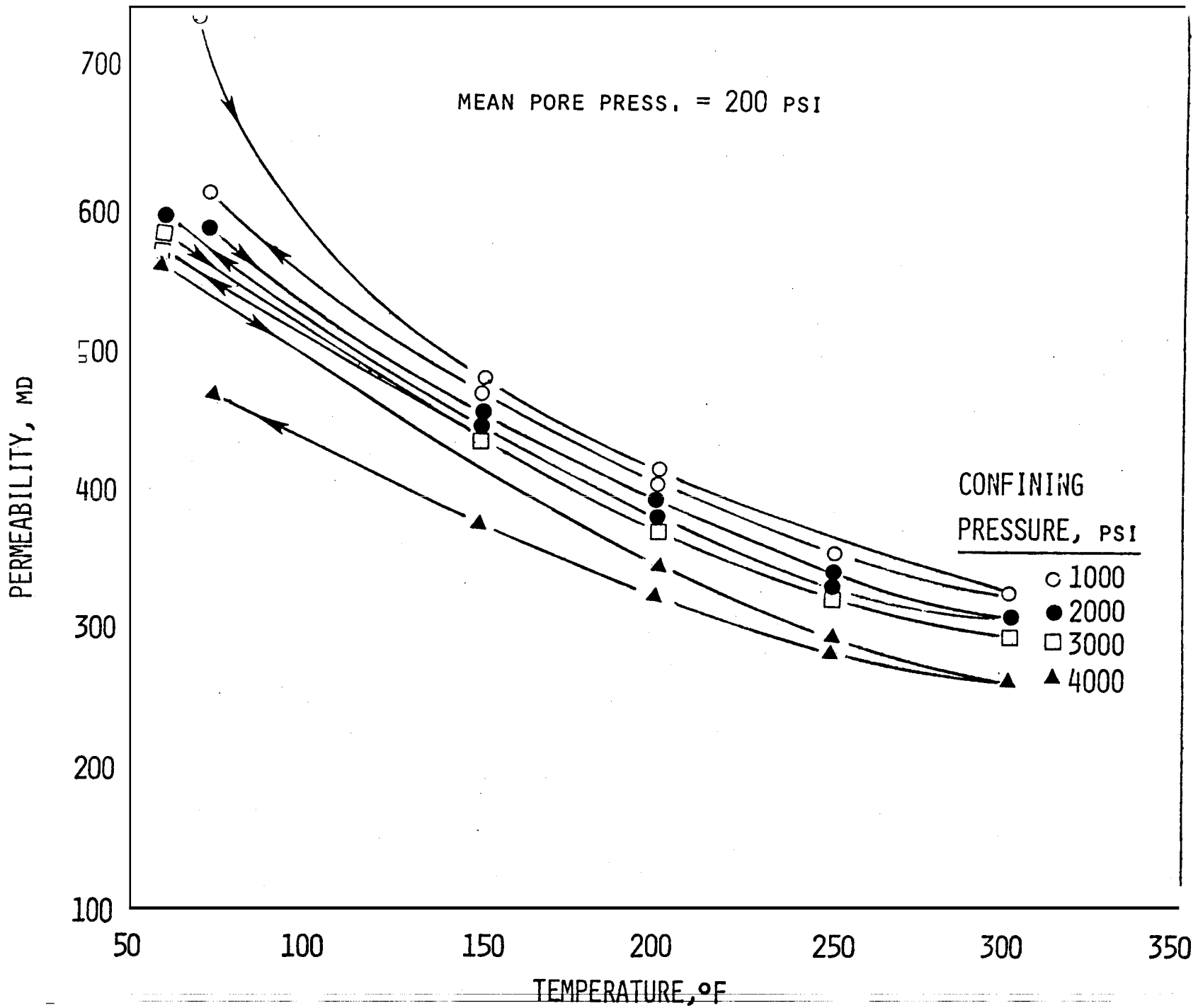

Fig. 13. Water Permeability vs. Temperature, Massillon Sandstone Core No. 3

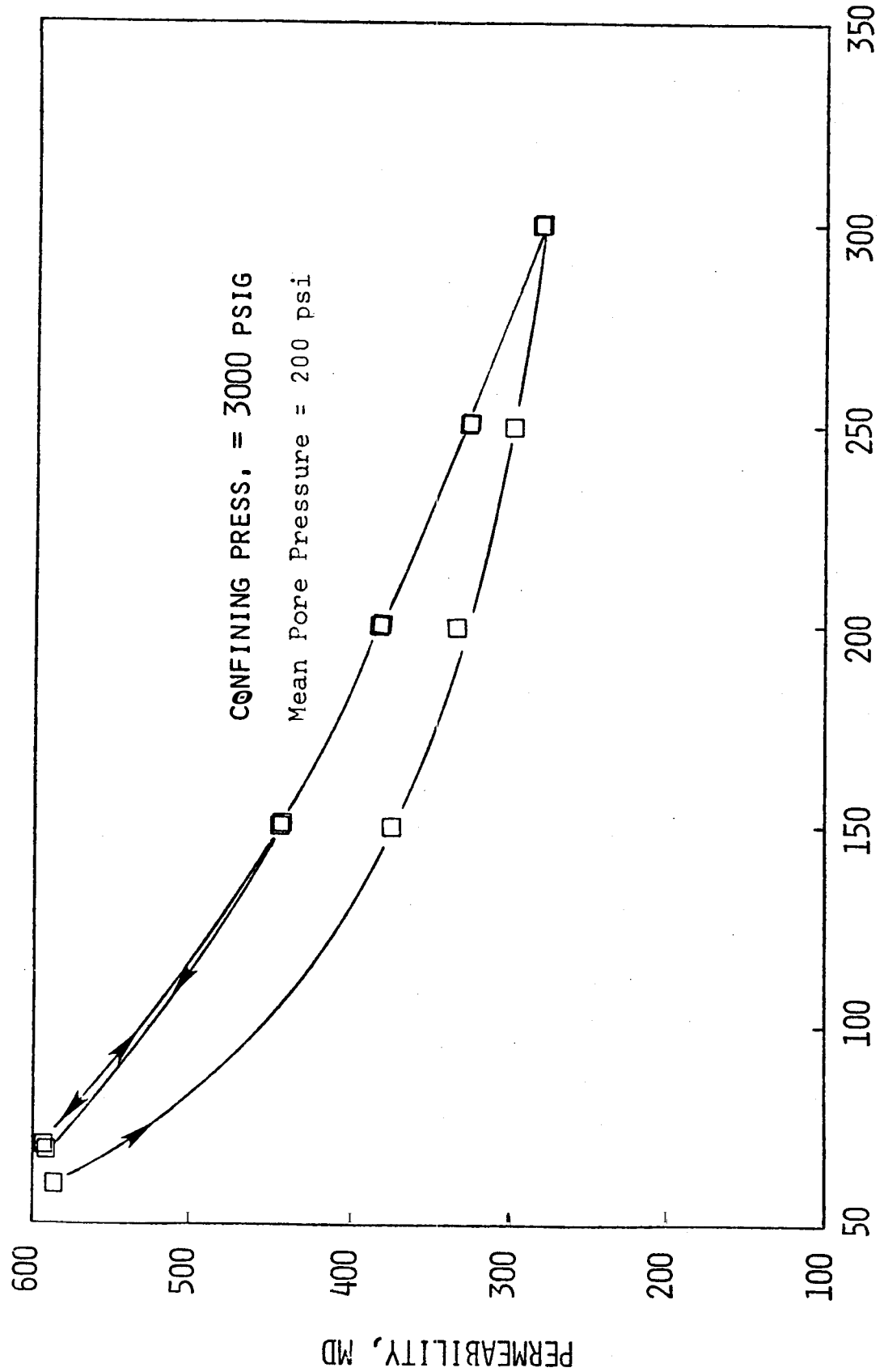

Fig. 14. Water Permeability vs. Temperature, at a Constant Confining Pressure of 3000 psig, Massillon Sandstone Core No. 3

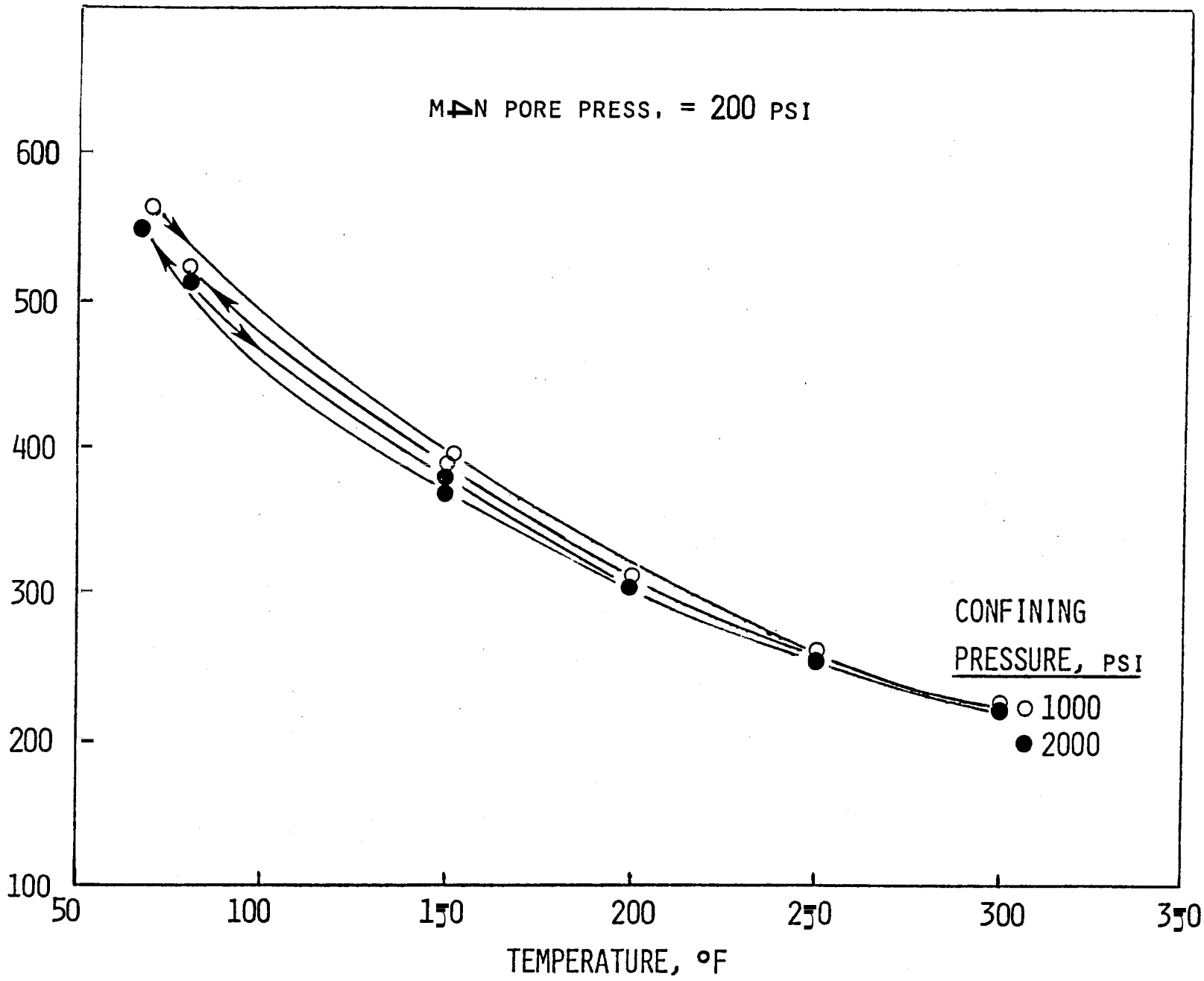

Fig. 15. Water Permeability vs. Temperature, Massillon Sandstone Core No. 4

-46-

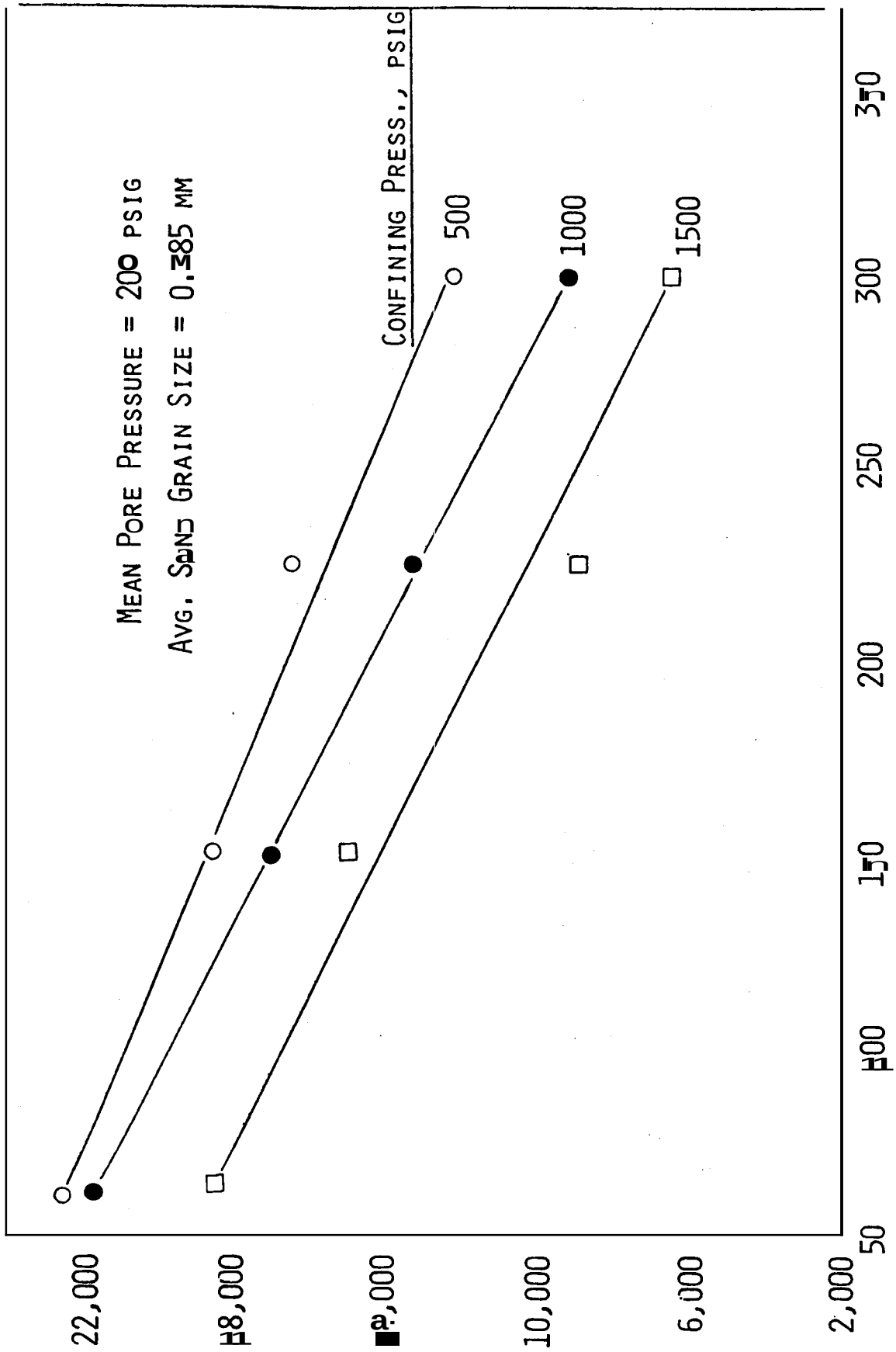

Fig. 16. Water Permeability vs. Temperature, Unconsolidated Ottawa Silica Sand Core No. 14

decreased with an increase in confining pressure. The rate of change was -0.5 md/°F at all levels of confining pressure. As the absolute permeability of this core was very high, 22,000 md at 500 psig confining pressure, the average sand grain size was reduced for the next experiment. See Ref. 26 for methods of control of permeability and porosity of synthetic sands.

6.2 Gas Flow

Gas flow experiments were conducted at three different temperature levels and a range of confining pressures. Absolute permeabilities were measured with nitrogen flow under conditions of viscous flow and graphed as a function of the reciprocal mean pressure on a conventional Klinkenberg graph. One run was conducted in the visco-inertial flow region for a consolidated sandstone. Details of the analysis of this gas flow data are given in Table 9 and in Appendix (section 9.3-2). In all cases, the absolute permeabilities at different temperatures but for the same confining pressure, extrapolated to the same infinite pressure value. The slopes of these graphs are, however, probably not true Klinkenberg slip coefficients. The high slopes are a result of the effects of a combination of both slip and mean pore pressure-confining pressure stress effects on permeability. Although the confining pressure was held constant at 1000 psi or more, the pore pressure changed from nearly atmospheric to several hundred psi for each series of runs. Determination of slip coefficients was not a major objective of this study. The valuable information from these graphs is that temperature has no apparent effect on absolute permeability to gas.

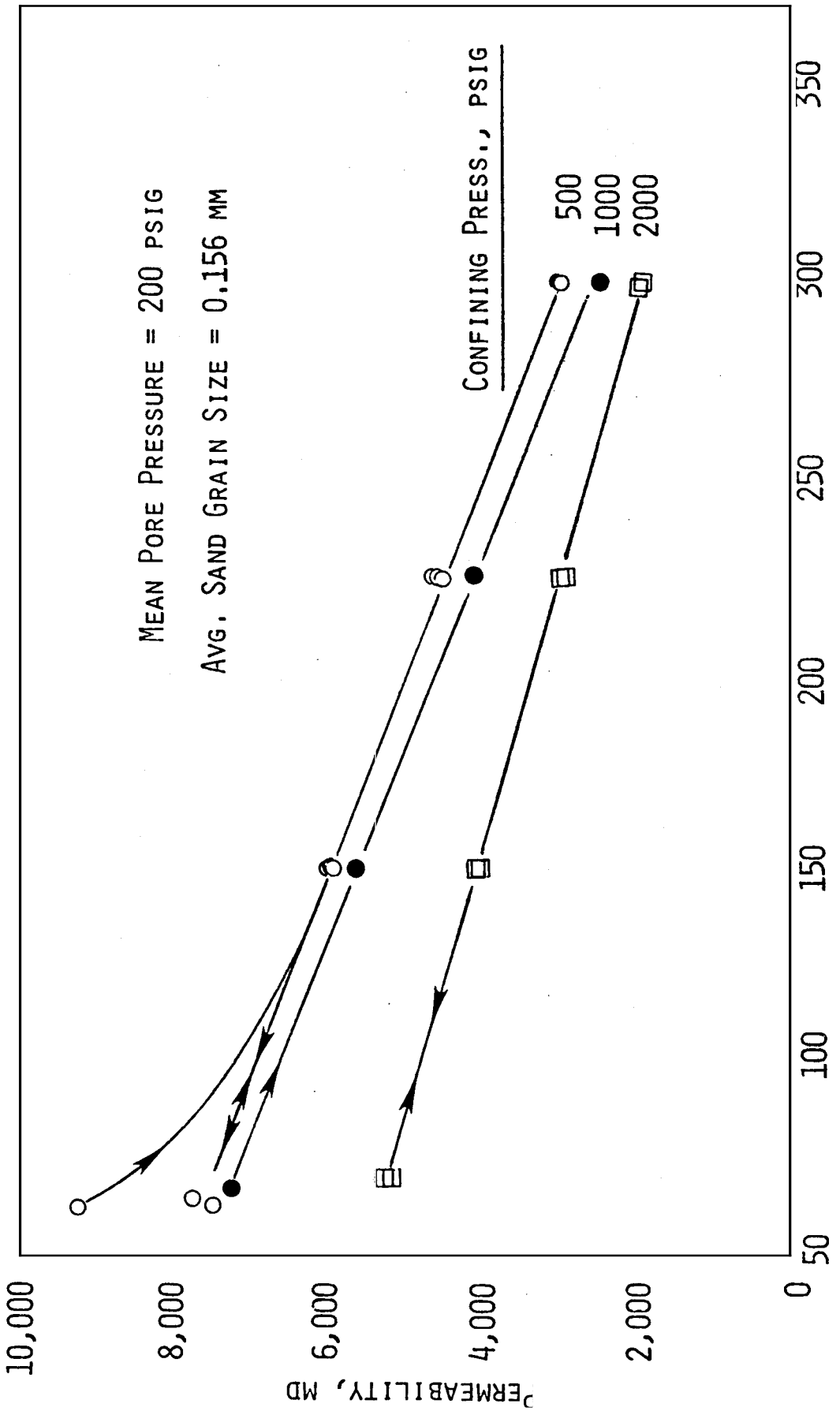

Fig. 17. Water Permeability vs. Temperature, Ottawa Silica Sand Core No. 15

6.2-1 Consolidated Sandstones: The results of the first run in the viscous and visco-inertial flow regions on Massillon Consolidated Sandstone Core No. 5 are shown on Figs. 18 and 19, respectively. On Fig. 18, the Klinkenberg slip factors at 68, 150, and 250°F are 2.264, 3.587, and 4.351 psi, respectively. This shows that the apparent Klinkenberg slip factor depends upon temperature. The apparent permeabilities at different temperatures and pressures extrapolated to the same value of 960 md and agree reasonably with the visco-inertial analysis value of 932 md shown on Fig. 19. The turbulence factor β, which may be obtained from Fig. 19, was 1.7×10^7 ft^{-1}, and is in agreement with a correlation proposed in Ref. 27. The confining pressure was held constant at 1000 psi in these runs.

Another series of experiments was conducted on Massillon Sandstone Core No. 6 at room, 150°F, and 250°F temperature levels and at confining pressures of 1000, 3000, and 4000 psig. Results are shown on Figs. 20-22, and are similar to those of Fig. 18. Absolute permeability decreased with an increase in confining pressure; and at the same level of confining pressure, the apparent permeabilities extrapolated to the same infinite pressure value apparent slip factors at room and 150°F temperature levels were essentially the same for all levels of confining pressure, but higher at 250°F temperature.

The values of absolute permeabilities obtained with nitrogen flow and water flow for the consolidated sandstone cores were different. Permeabilities to water at room temperature ranged between 550 md and 450 md for all of the

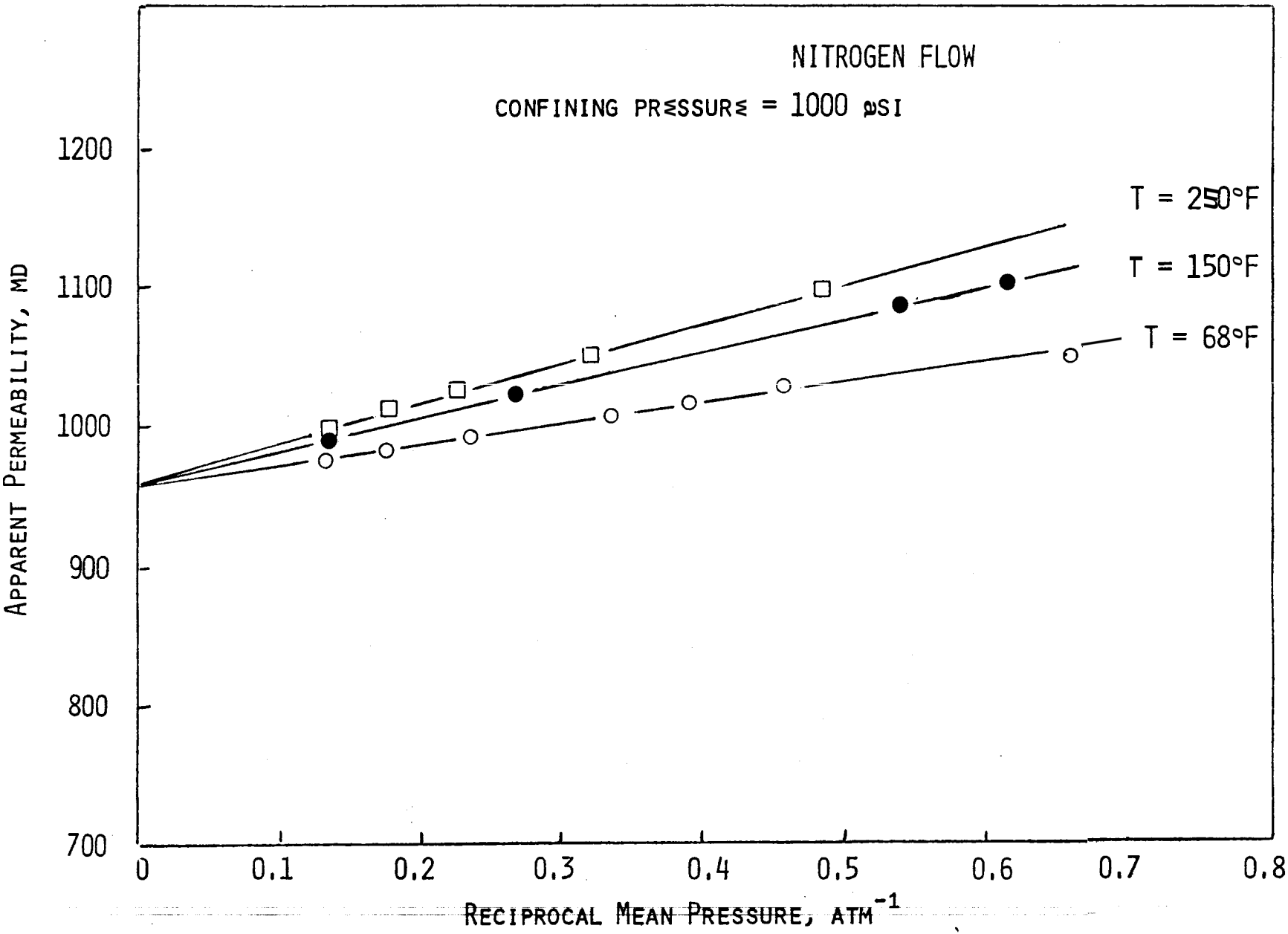

Fig. 18. Apparent Permeability vs. Reciprocal Mean Pressure at Several Temperatures for Massillon Sandstone Core No. 5

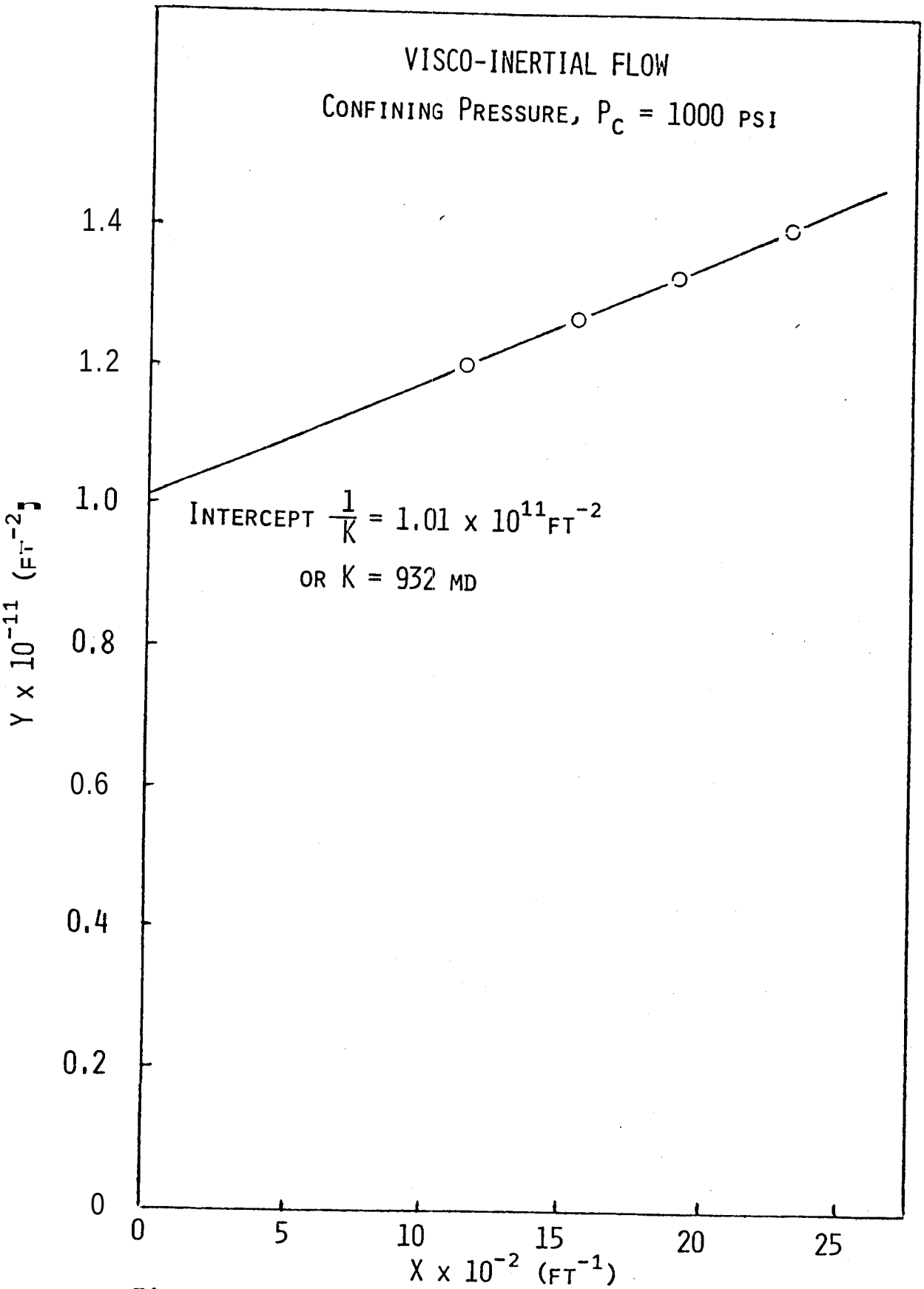

Fig. 19. Modified Visco-Inertial Graph, Massillon Sandstone Core No. 5 with Nitrogen Flow

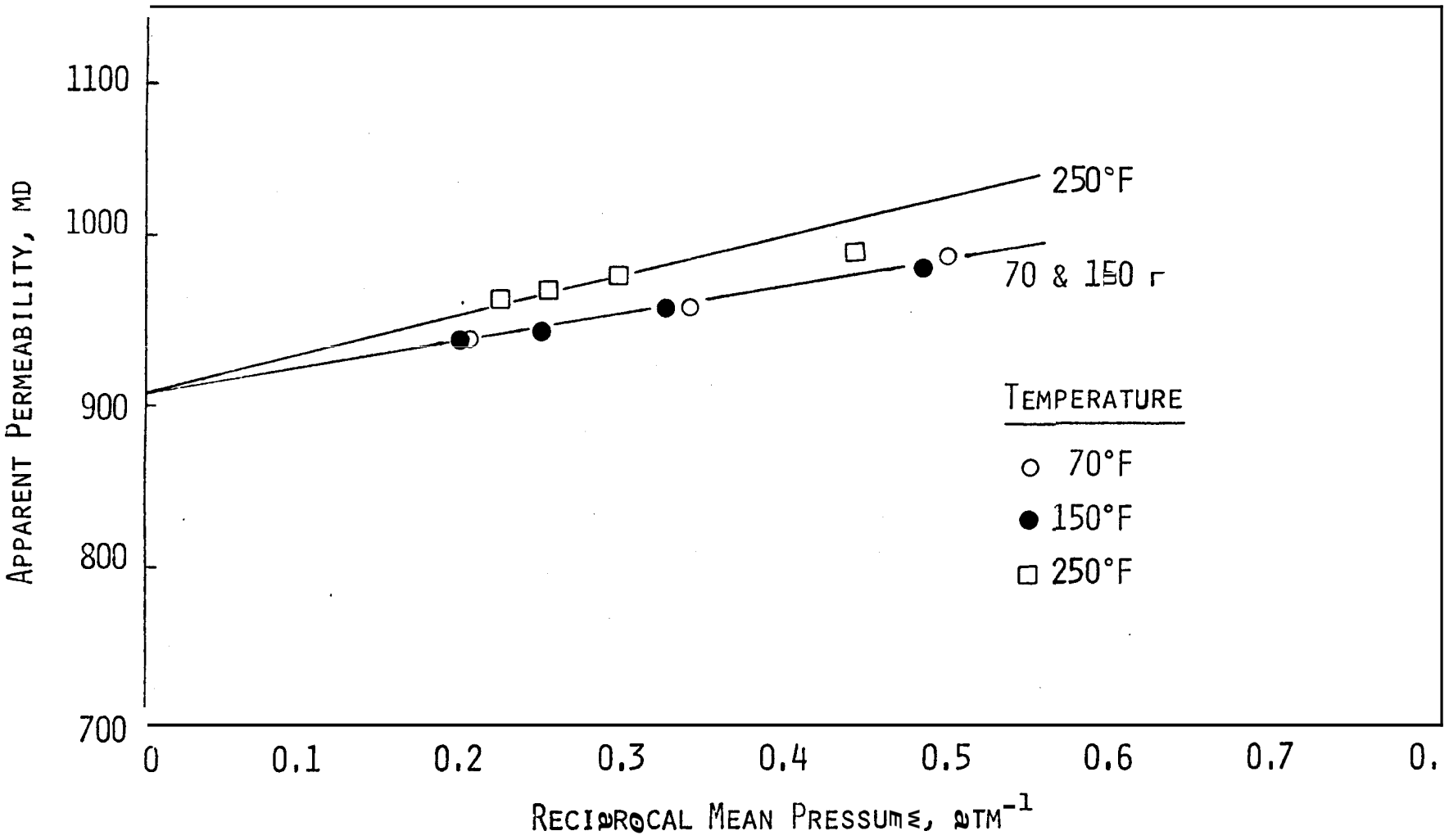

Fig. 20. Apparent Permeability vs. Reciprocal Mean Pressure at Several Temperatures for Massillon Sandstone Core No. 6, Confining Pressure = 1000 psig

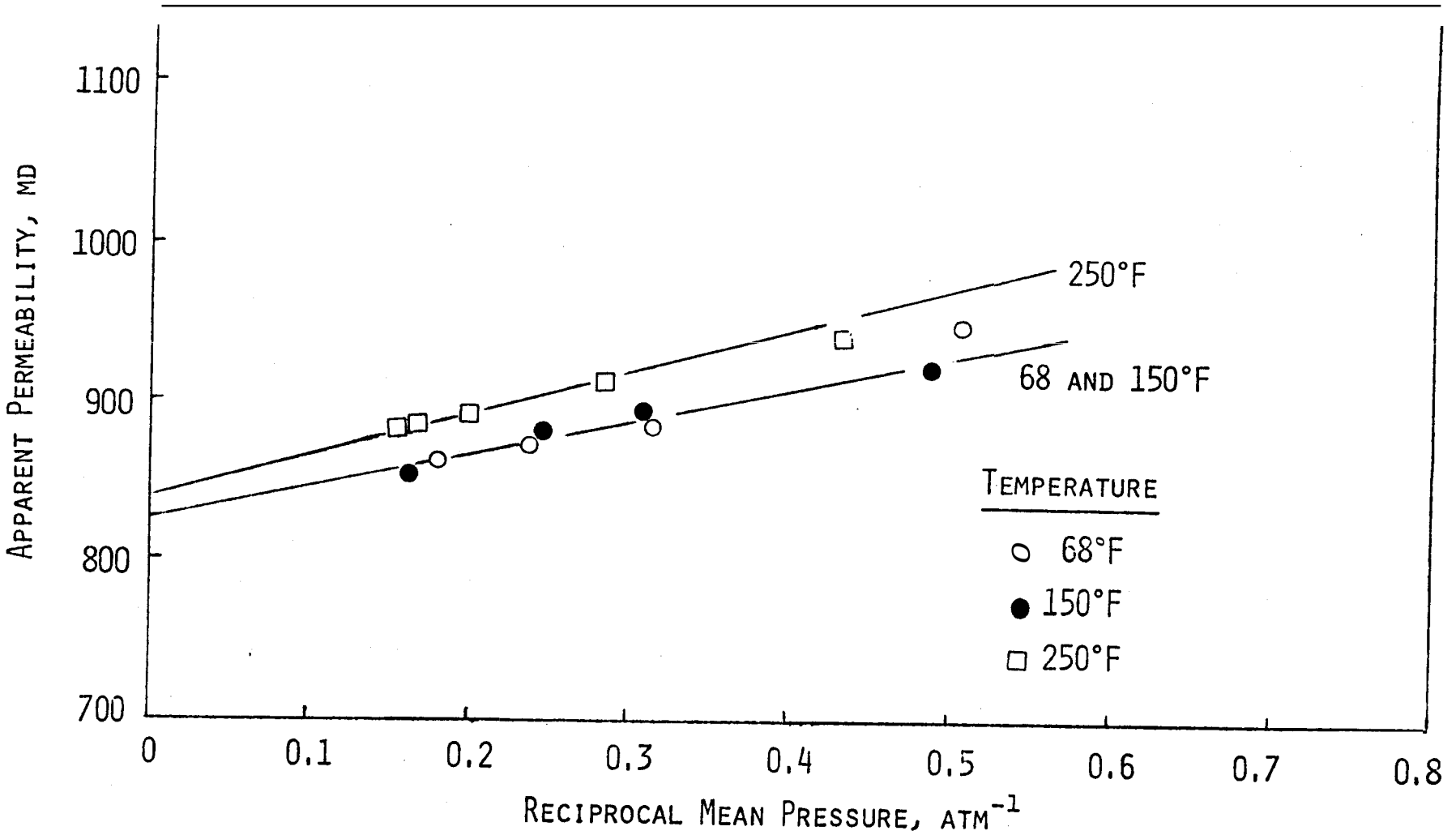

Fig. 21. Apparent Permeability vs. Reciprocal Mean Pressure at Several Temperatures for Massillon Sandstone Core No. 6, Confining Pressure = 3000 psig

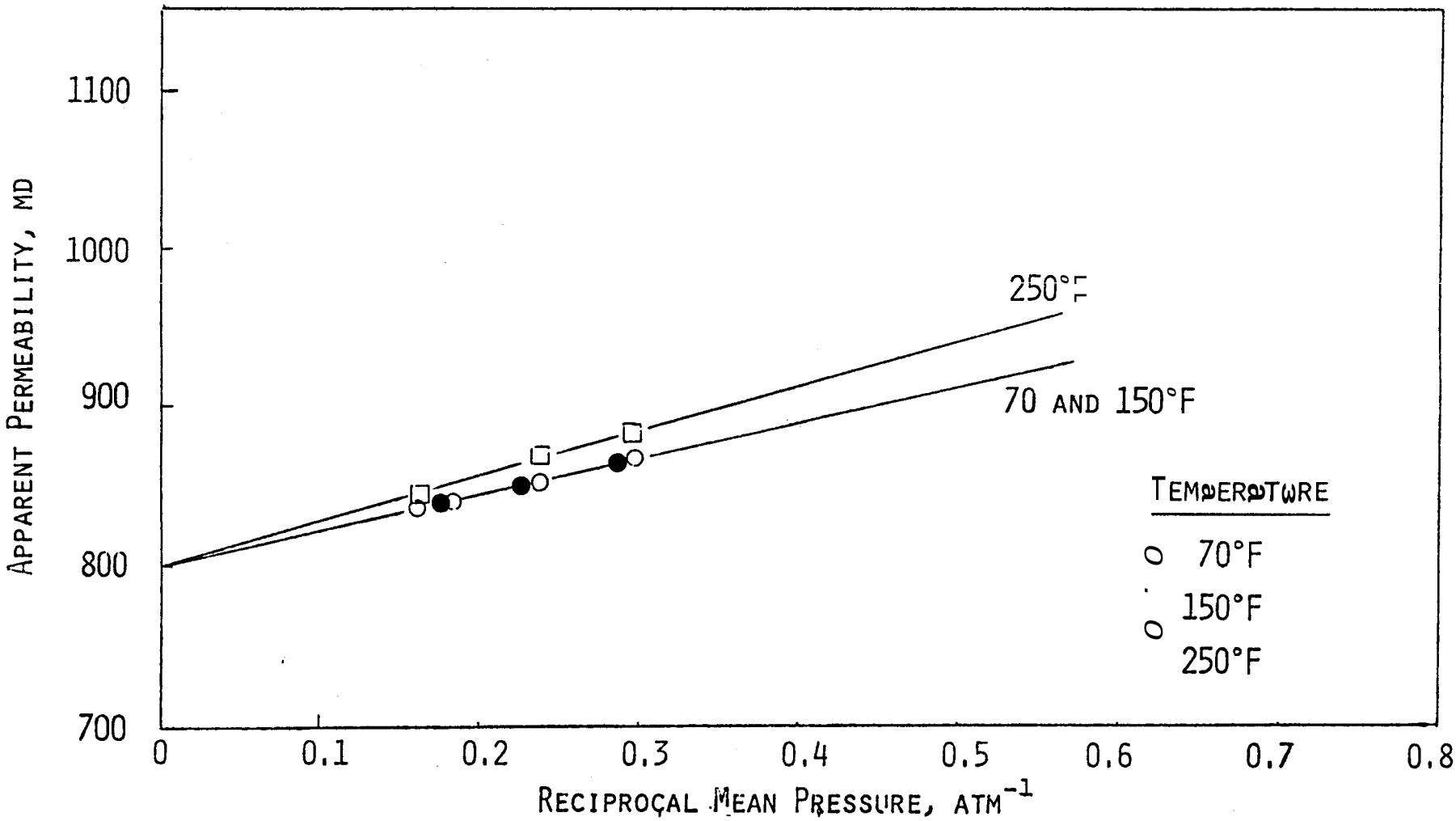

Fig. 22. Klinkenberg Permeability vs. Reciprocal Mean Pressure at Several Temperatures for Massillon Sandstone Core No. 6, Confining Pressure = 4000 psig

confining pressure levels, while absolute permeabilities to nitrogen were considerably higher and ranged from 960 md to 800 md for the same conditions. This suggests that the phenomena causing the permeability reduction with water flow at room temperature may also be responsible for the permeability reduction at high temperatures. The Massillon Sandstone has a low clay content, and had been fired at 500°C.

6.2-2 Unconsolidated Sand: Fig. 23 shows results obtained with fired silica sand. A 2000 psig confining pressure was applied, and the temperature levels used were 68°F, 150°F, and 250°F. The results were similar to those for the consolidated sandstones.

Permeability to water was also measured for this core. While the extrapolated absolute permeability to nitrogen was 4,260 md, the permeability to water was only 2,127 md at room temperature.

6.3 Oil Flow

Because of the difference between the results obtained at elevated temperatures with water flow and gas flow, similar experiments were run with another fluid. Chevron White Oil No. 3 was chosen for its higher viscosity and its non-polar characteristics, as opposed to water, which is an intermediate viscosity polar fluid and may interact with the rock surface. Experiments (see Ref. 1) had already been carried out with Chevron White Oil No. 15, which is very viscous. As in water flow or gas flow experiments, the combined effect of temperature and overburden pressure was investigated.

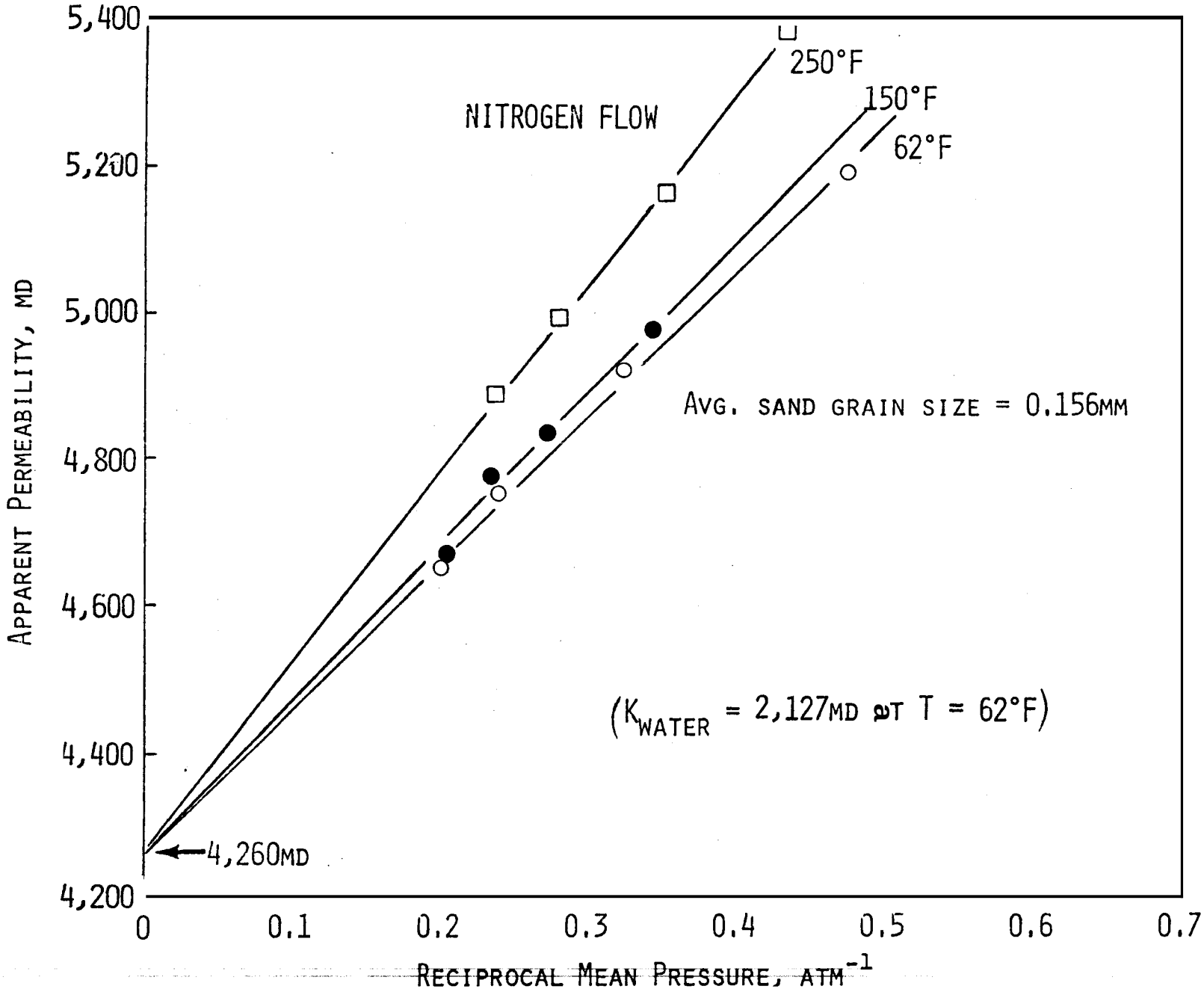

Fig. 23. Klinkenberg Permeability vs. Reciprocal Mean Pressure at Several Temperatures for Ottawa Silica Sandcore No. 16, Confining Pressure = 2000 psig

Figs. 24 and 25 show the results with oil flow for cores No. 10 and 11. Oil flow was conducted only on consolidated sandstones. Absolute permeability to oil was affected by confining pressure, as expected, but there was only a slight decrease in absolute permeability to oil with temperature increase. Hysteresis effects in cooling cycles were more pronounced at high confining pressures of 3000 psi and 4000 psi.

Permeability levels at room temperature agree closely with those obtained with nitrogen flow. The absence of rock-oil interaction is believed to be responsible for the difference between water and oil permeabilities. This suggests a definite interaction between water and sandstone, consolidated or unconsolidated.

6.4 2-Octanol Flow

In view of the results with water, it appeared useful to run similar experiments with another polar liquid. 2-octanol alcohol was chosen.

Experiments were conducted with commercial grade 2-octanol, and the results are presented in Fig. 26. The unconsolidated Ottawa Silica Sandcore used was fired at 500°C. The average sand grain size was 0.156 mm. The confining pressure affected the absolute permeability as expected, but temperature appeared to cause a small increase in absolute permeability. In addition, there was a permanent reduction in absolute perneability on each cooling cycle. These results are dramatic when compared to the water data on Figs. 16 and 17.

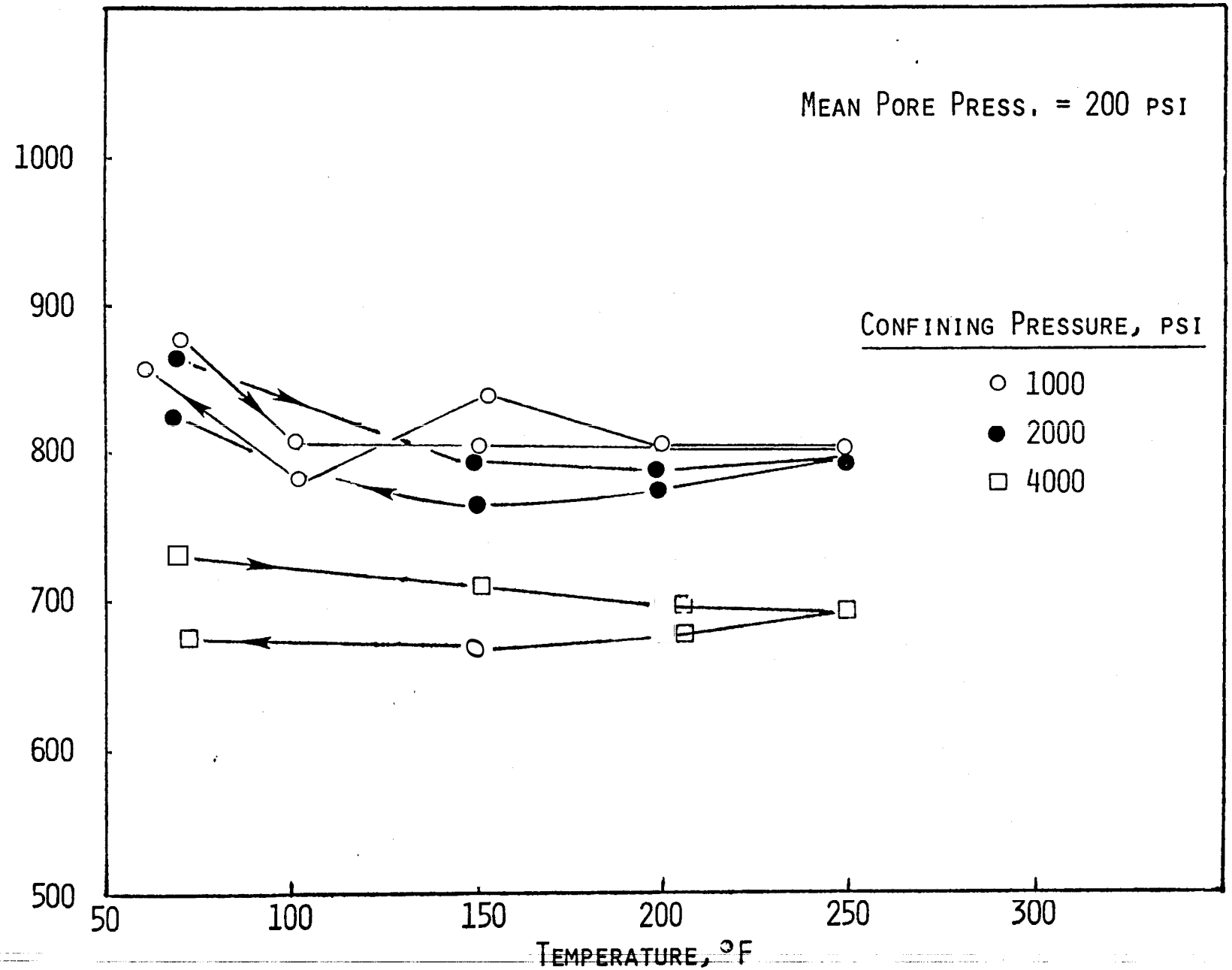

Fig. 24. Oil Permeability vs. Temperature for Massillon Sandstone Core No. 10

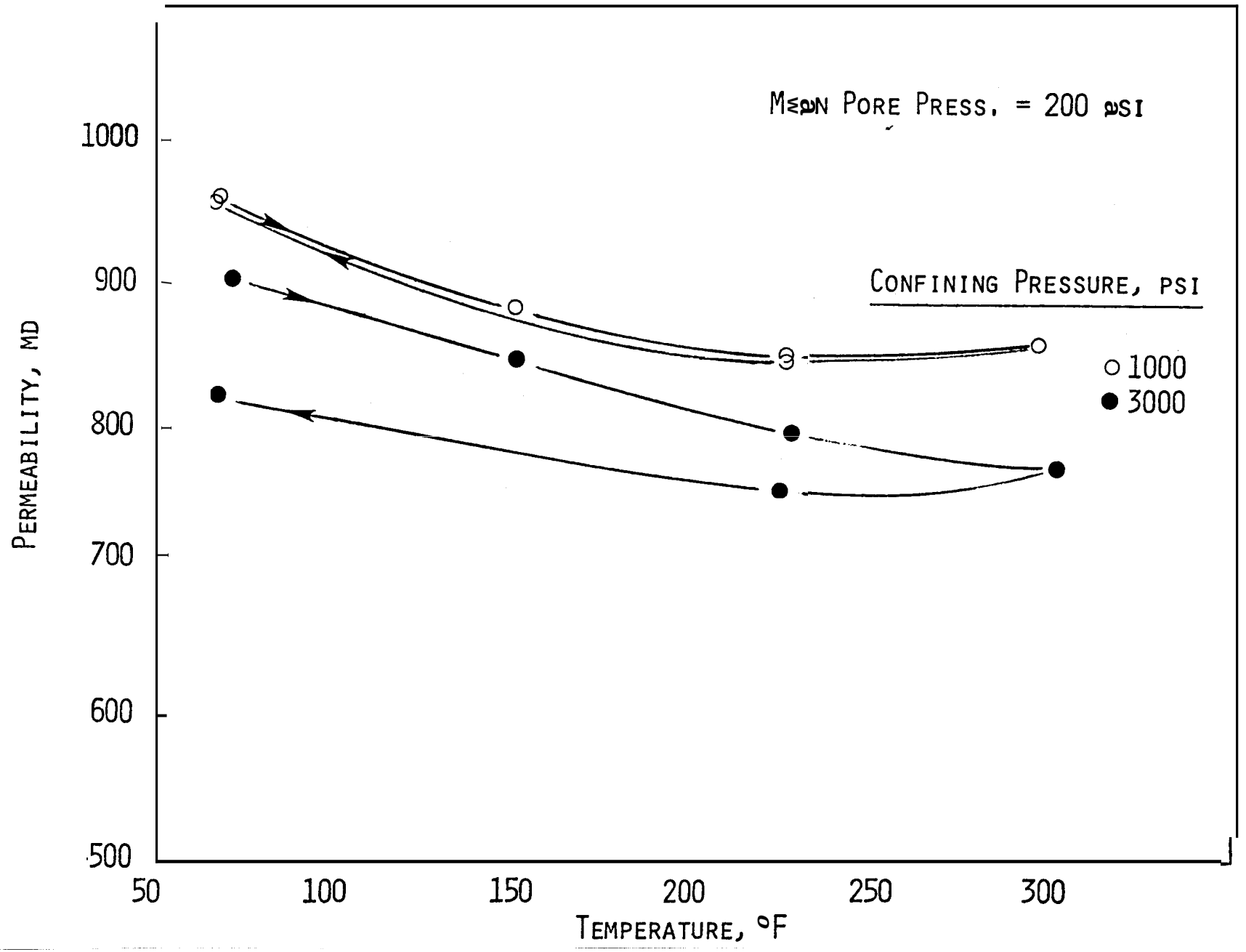

Fig. 25. Oil Permeability vs. Temperature for Massillon Sandstone Core No. 11

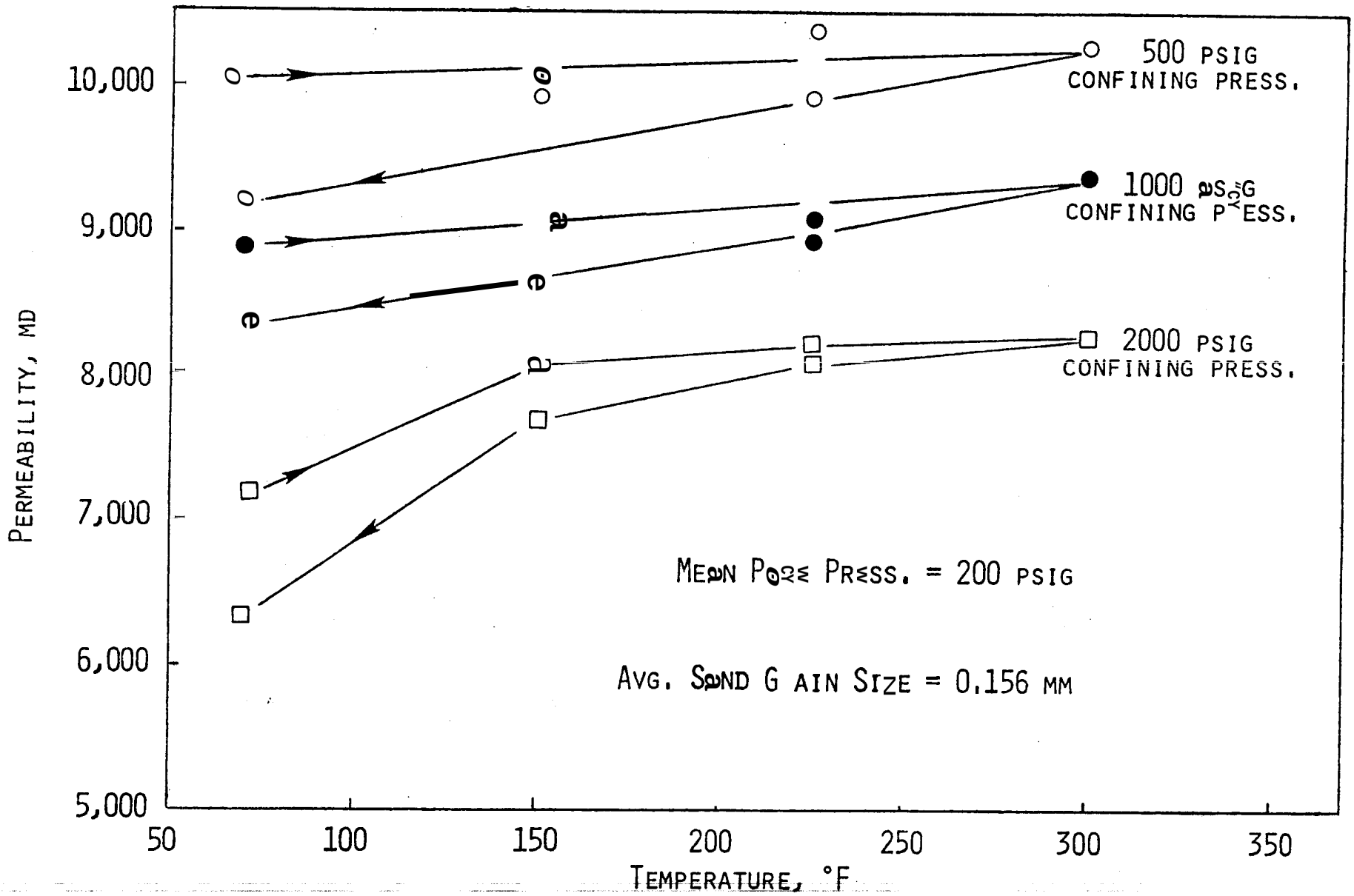

Fig. 26. 2-Octagonal Permeability vs. Temperature for Unconsolidated Ottawa Sand Core No. 17

The slight increase in permeability to octanol with temperature increase for both heating and cooling runs emphasizes the importance of the decrease in k with temperature increase for water. Recent discussions between Ramey and Dreher (Marathon Oil Co., Denver) revealed that octanol often behaves more like an oil than an aqueous wetting phase in sandstones. In retrospect, it might have been better to have selected bopropyl alcohol (IPA) as the second polar substance. It is recommended that IPA be considered for future studies.

6.5 Discussion

Cassé[1] concluded that clay-water interactions may have been one reason for the effect of temperature level upon absolute permeability to water for sandstones he observed. Grim[30,31] presented a comprehensive review of the mechanisms involved in clay-water interactions. Because the rocks used in this work were totally or nearly clay-free, clay-water interaction is considered responsible for only a minor role in the phenomenon observed in this study.

It is almost certain that water-cilica interactions are responsible for the major effects observed with water. In addition to the results of this study, Grunberg and Nissan[13] used aqueous solutions (including Amyl Alcohol) with Jena Glass Filters of low permeability (160 md at room temperature) and found a linear decrease in absolute permeability with an increase in temperature.

Fluid flow mechanisms[32] often fit two categories: (1) mechanisms which are essentially mechanical in nature, the

flow depending on the bulk properties of the fluids concerned and upon the mechanical forces exerted upon the fluid bodies; and (2) mechanisms which are essentially molecular in character, the flow depending largely on the motion of the individual molecules, the molecular weight, the collision cross-section, the mean free path, rock-fluid attractive forces, etc., rather than upon the density, pressure viscosity, etc., of the fluid in bulk. The latter mechanisms may be dominant in the case of the effect of temperature upon water flow in sandstones under pressure.

Surface attractive forces between silica and water molecules may be large enough to lead to chemi-sorption. In such a case, the adsorbate molecules become practically a part of the solid surface and, compared with other molecules in the liquid, such chemi-sorbed molecules may be largely immobilized. The effective cross-section under viscous flow could then be different for water from the other fluids tested. Increases in temperature[33] seem to increase this effect from the results of this study. An exhaustive literature survey indicated no known phenomena capable of explaining the magnitude of the effects observed in this study. It is believed that a major, and heretofore unsuspected attraction between water and silica has been discovered. It is possible that this attraction is essentially responsible for the large temperature effects on practical irreducible water saturation and relative permeabilities[34,16,35], and on capillary pressures[36-38] and resistivity previously reported.

If a strong attraction between water and silica is the major temperature effect, several new experiments with gas-oil flow in sandstones will show no temperature effect, while gas-water flow in sandstone will depend on temperature. In addition, experiments of any sort in limestones should not depend strongly on temperature.

7. CONCLUSIONS AND RECOMMENDATIONS

Experimental results indicate that the absolute permeability to water for confined sandstones is strongly temperature dependent. The absolute permeability of sandstones to other fluids (nitrogen, mineral oil, octanol) is either, unaffected or only slightly affected by temperature level. Temperature increase has the effect of decreasing the absolute permeability to water for sandstones remarkably.

Temperature change has little or no effect on the absolute permeability of sandstones to nitrogen, mineral oil, or octanol. In the case of water flow, permeability reductions of up to 60% were observed over a temperature range of 70-300°F.

Regardless of the type of flowing fluid, the level of confining pressure affected absolute permeability in the same manner, i.e., permeability decreased with increasing confining pressure. For water flow experiments, increasing the confining pressure had the additional effect of intensifying the temperature dependence of absolute permeability in many cases (but not all).

In the light of the results obtained, it seems that unsuspected fluid-solid surface attractive forces between water molecules and silica were largely responsible for the major effects observed. The following recommendations appear pertinent.

It is recommended that the results obtained by Grunberg and Nissan[13] be rechecked for the same aaueous solutions and for confined porous media. It is also recommended that experiments be repeated for higher temperatures and confining pressures.

Since octanol behaves more like an oil than an aqueous wetting phase in sandstones, it is recommended that isopropyl alcohol be used as the second polar substance for future studies. Results from such studies may help to explain whether the decrease in water permeability with increasing temperature is due to the polarity of water.

If a strong attraction between water and silica causes the temperature effect, experiments designed to isolate water and/or silica will be enlightening. Experiments with water flow in limestones should not depend strongly on temperature. In addition, experiments with gas-oil flow in sandstones may show no temperature effect while gas-water flow in sandstone will depend on temperature.

8. REFERENCES

1. Cassé, F.J.: "The Effect of Temperature and Confining Pressure on Fluid Flow Properties of Consolidated Rocks," Ph.D. Dissertation, Stanford University (1974).

2. Arihara, N.: "A Study of Non-Isothermal Single and Two-Phase Flow through Consolidated Sandstones," Ph.D. Dissertation, Stanford University (1974).

3. Greenberg, D.B., Cresap, R.S., and Malone, T.A.: "Intrinsic Permeability of Hydrological Porous Mediums: Variation with Temperature," Water Resources Research (Aug. 1968), 4, No. 4, 791.

4. Muskat, M.: Flow of Homogeneous Fluids through Porous Media, McGraw-Hill Book Company, Inc., 1937, Ch. 11.

5. Fancher, G.H., Lewis, J.A., and Barnes, K.: "Some Physical Characteristics of Oil Sands," Ind. Eng. Chem., 25: 1139 (1933).

6. Geertma, J.: "Estimating the Coefficient of the Inertial Resistance in Fluid Flow through Porous Media," Soc. Pet. Eng. Jour. (Oct. 1974), 445.

7. Amyx, J.W., Bass, D.M., Jr., and Whiting, R.L.: Petroleum Reservoir Engineering, McGraw-Hill Book Company, Inc., 1960, Ch. 2.

8. Kundt, A., and Warburg, E.: Poggendorf's Ann. Physik, pp 155, 337, 525.

9. Klinkenberg, L.J.: "The Permeability of Porous Media to Liquids and Gases," Drill. and Prod. Prac., API (1941), 200.

10. Forchheimer, P.: "Hydraulik," Leipzig and Berlin, Ch. 15 Sections 116-118, Druck and Verlag von B.G. Teubner (1914).

11. Cornell, D., and Katz, D.L.: "Flow of Gases through Consolidated Porous Media," Ind. Eng. Chem. (1953), Vol. 45, p. 2145.

12. Dranchuk, P.M., and Kolada, L.J.: "Interpretation of Steady Linear Visco-Inertial Gas Flow Data," Jour. Can. Pet. Tech. (1968), 7, No. 1, p. 36.

13. Grunberg, L., and Nissan, A.H.: "The Permeability of Porous Solids to Gases and Liquids," Jour. of Inst. of Pet. (1953), 29, No. 236, p. 193.

14. Calhoun, J.C., Jr., and Yuster, S.T.: "A Study of the Flow of Homogeneous Fluids through Ideal Porous Media," Drill and Prod. Prac., API (19461, 335.

15. API RP 27: "Recommended Practice for Determining Permeability of Porous Media," Am. Pet. Inst. (Aug. 1956).

16. Weinbrandt, R.M. : "The Effect of Temperature on Relative Permeability," Ph.D. Dissertation, Stanford University (1972).

17. Wilhelmi, B., and Somerton, W.H.: "Simultaneous Measurement of Pore and Elastic Properties of Rocks under Triaxial Stress Conditions," Soc. Pet. Eng. Jour. (Sept. 19671, 240, 283.

18. Fatt, I., and Davis, D.H.: "Reduction in Permeability with Overburden Pressure," Trans., AIME (1952), 195, 329.

19. Gray, D.H., Fatt, I:, and Bergamini, G.: "The Effect of Stress on Permeability of Sandstone Cores," Soc. Pet. Eng. Jour. (June 1963), 95.

20. Zoback, M.D., and Byerlee, J.D.: "Permeability and Effective Stress," Amer. Assoc. Pet. Geol. Bull., 59 (1) (1975a), 154.

21. Somerton, W.H. , Mehta,, M.M., and Dean, G.W. : "Thermal Alteration of Sandstones," J. Pet. Tech. (May 1965), 589.

22. Wyble, D.O.: "Effect of Applied Pressure on the Conductivity, Porosity, and Permeability of Sandstones," Trans. AIME (1958), 213, 430.

23. Meyer, C.A., McClintock, R.B., Silvestri, G.J., and Spencer, R.C., Jr.: 1967 ASME Steam Tables, Am, Soc. Mech. Engrs., 2nd ed., New York, N.Y., 1968.

24. ASTM-IP-Petroleum Measurement Tables, ASTM, Philadelphia (1952).

25. Perry, J.H. : Chemical Engineer's Handbook, McGraw-Hill Book Company, Inc. (1969), pp. 23-10.

26. Larman, H.J. : "Variations in Permeability and Porosity of Synthetic Oil Reservoir Rock--Methods of Control," Soc. of Pet. Eng. Jour. (Dec. 1965), 329.

27. Katz, D.L., and Coats, K.H.: Underground Storage of Fluids, Ulrich's Books, Inc., Ann Arbor, Michigan (1968).

28. Jones, S.C.: "A Rapid, Accurate Unsteady-State Klinkenberg Permeameter," Soc. Pet. Eng. Jour. (Oct. 19721, 483.

29. Sax, N.I.: Dangerous Properties of Industrial Materials, Reinhold Publishing Corporation (1963).

30. Grim, R.E.: Applied Clay Mineralogy, McGraw-Hill Book Company, Inc. (1962).

31. Grim, R.E.: Clay Mineralogy, McGraw-Hill Book Company, Inc. (1968).

32. Flood, E.A.: "Influence of Surface Forces on Flow of Fluids through Capillary Systems," Highway Research Board, Spec. Rep. No. 40 (19581,

33. Bartell, F.E., Thomas, T.L., and Fu, Y.: "Thermodynamics of Adsorption from Solution, iv. Temperature Dependence of Adsorption," Jour. of Phys. Chem. (1951), 55, 1456,

34. Poston, S.W., Ysrael, S., Hossain, A.K.M.S., Montgomery, E.F., 111, and Ramey, H.F., Jr.: "The Effect of Temperature on Irreducible Water Saturation and Relative Permedbility of Unconsolidated Sands," Soc. of Pet. Eng. Jour. (June 19701, 171.

35. Weinbrandt, R.M., Cassé, F.J., and Ramey, H.J., Jr.: "The Effect of Temperature on Relative and Absolute Permeability of Sandstones," Soc. of Pet. Eng. Jour. (Oct. 1975), 376.

36. Sinnokrot, A.A., Ramey, H.J., Jr., and Marsden, S.S., Jr.: "Effect of Temperature Level upon Capillary Pressure Curves," Soc. of Pet. Eng. Jour. (March 1971), 13.

37. Okandan, E., Marsden, S.S., Jr., and Ramey, H.J., Jr.: "Capillary Pressure and Contact Angle Measurements at Elevated Temperatures," presented at AIChE Meeting, Tulsa, Oklahoma, March 12, 1974.

38. Sanyal, S.K., Ramey, H.J., Jr., and Marsden, S.S., Jri.: "The Effect of Temperature on Capillary Pressure Properties of Rocks," SPWLA 14th Annual Logging Symposium (May 1973).

39. National Research Council of U.S.A.: "International Critical Tables of Numerical Data, Physics, Chemistry and Technology," Vol. I-VII, 1933.

9. APPENDICES

9.1 List of Tabulated Data

Table 1. Density and Viscosity of Water vs. Temperature (from Steam Tables[25])

Pressure = 200 psig

Temperature °F	Density gm/cc	Viscosity cp
60	0.9990	1.100
100	0.9931	0.679
150	0.9803	0.426
200	0.9632	0.300
250	0.9423	0.228
300	0.9180	0.183
350	0.8904	0.152

Table 2. Viscosity of Nitrogen vs. Temperature

Pressure = 14.7 psia

Temperature °F	Temperature °K	Viscosity cp
60	288.7	0.01739
100	310.9	0.01839
150	338.7	0.01959
200	366.5	0.02074
250	394.3	0.02185
300	422.0	0.02291

$$\mu_{N_2} = \frac{13.85(10^{-4})\cdot 1.5}{102+T}, \quad T \text{ in } {}^{\circ}K$$

$${}^{\circ}K = \frac{T({}^{\circ}F)-32}{1.8} + 273.16$$

Table 3. Viscosity of Chevron Oil No. 3 vs. Temperature

Pressure = 200 psig

$$\mu_T = \alpha_T \frac{\Delta p}{q}$$

where $\alpha_{\text{T}} = 05113 \left[1 + 2\ 07 \times 10^{-5}\ (\text{T} - 70^{\circ}\text{F})\right]$

Temp. °F	(1) Oil Density ρ, gm/cc	(2) α_T cp-sec / psi-cc	(3) Δp psi	(4) Flow Rate q, cc/sec	(5) (2)x(3)/(4) Oil Viscosity μ, cp	(6) (5)/(1) Visc. u, cst
66	0.84883	0.05110	3.96	0.005719	35.4	41.7
70	0.8475	0.05113	4.0	0 006451	31.5	37.3
80	0.84415	0.05114	3.95	0.008873	22.8	27
100	0.83743	0.05117	3.93	0 01449	13.9	16.6
150	0.8208	0.05124	3.9	0 036586	5.5	6.7
200	0.8046	0.05131	3.95	0.0 0854	2.96	3.7
250	0.7886	0.05138	3.90	0 10746	1.86	2.36

Table 4. Density of 2-Octanol vs. Temperature

Pressure = Atmospheric

Temperature °F	Total Weight (Pycnometer + Octanol) gm.	2-Octanol Weight gm.	2-Octanol Density gm/cc
150	56.7370	18.8828	0.7868
125	56.9720	19.1178	0.7966
100	57.2090	19.3548	0.8065
80	57.3655	19.5113	0.8140
66	57.5330	19.6788	0.8200

Dry Pycnometer Weight = 37.8542 gm

Pycnometer Volume = 24.00 cc

Table 5. Viscosity of 2-Octanol vs. Temperature

Pressure = **200 psig**

Temp. °F	α_T cp-sec / psi-cc	Δ_P psi	q cc/sec	μ cp
66	0.05112	1.50	0.00725	10.58
100	0.05117	1.25	0.01266	5.05
150	0.05124	1.00	0.02222	2.306
200	0.05131	1.00	0.04000	
250	0.05138	0.75	0.04494	0.87
300	0.05144	0.75	0.0625	0.614

$$\mu_T = \alpha_T \frac{\Delta p}{q}$$

where $\alpha_T = .05113 \left[1+2.67 \times 10^{-5} \ (T-70^{\circ}F) \right]$

Table 5 Flow Data for Massillon Sandstone Core No. 2, Water flow

Mean Pore Pressure = 200 psig

L = 5.2325 cm

A = 4.837 cm^2

$$k = \frac{14.7}{\Delta p} \times 10^3 \times \frac{L}{A} \times \mu \times \frac{W}{\rho}$$

Run No.	T_a °F	T_c °F	Δp psi	w g/sec	ρ g/cc	P_c psig	μ cp	k md
1	69	69	0.50	0.0177	0.9981	1000	0.980	553
2	73	100	0.75	0.0383	0.9931	1000	0.679	555
3	74	150	0.40	0.0314	0.9803	1000	0.426	543
4	78	200	0.20	0.0206	0.9632	1000	0.300	509
5	74	250	0.15	0.0183	0.9423	1000	0.228	470
6	72	300	0.15	0.190	0.9180	1000	0.183	402
7	70	69	0.65	0.0194	0.9981	2000	0.970	461
8	76	150	0.50	0.0298	0.9803	2000	0.426	411
9	75	200	0.35	0.0268	0.9632	2000	0.300	379
10	74	240	0.20	0.0167	0.9467	2000	0.240	337
11	74	290	0.25	0.0249	0.9180	2000	0.190	326
12	70	71	0.65	0.0195	0.9979	3000	0.950	454
13	75	150	0.35	0.0204	0.9803	3000	0.426	404
14	72	200	0.30	0.0214	0.9632	3000	0.300	353
15	72	250	0.25	0.0207	0.9432	3000	0.228	318
16	80	300	0.20	0.0179	0.9180	3000	0.183	284
17	73	75	0.65	0.0195	0.9974	4000	0.900	430
18	74	150	0.35	0.0191	0.9803	4000	0.426	377
19	70	200	0.20	0.0142	0.9632	4000	0.300	351
20	73	250	0.15	0.0116	0.9432	4000	0.228	298
21	71	300	0.10	0.0083	0.9180	4000	0.183	262

Table 7. Flow Data for Massillon Sandstone Core No. 3, Waterflow

Mean Pore Pressure = 200 psig

L = 5.180 cm

A = 4.896 cm^2

$$k=\frac{14.7}{\Delta p}\times 10^3 \times \frac{L}{A}\times \mu \times \frac{w}{\rho}$$

Run No.	T_a °F	P_c °F	Δp psi	w g/sec	ρ g/cc	P_c psig	μ cp	md
1	72	72	0.40	0.0204	0.9978	1000	0.935	745
2	75	150	0.30	0.0205	0.9803	1000	0.426	462
3	71	300	0.20	0.0206	0.9180	1000	0.183	320
4	75	250	0.20	0.0185	0.9432	1000	0.228	349
5	72	200	0.24	0.0200	0.9632	1000	0.300	404
6	72	150	0.30	0.0208	0.9803	1000	0.426	470
7	72	72	0.48	0.0202	0.9978	1000	0.935	614
8	72	72	0.50	0.0200	0.9978	2000	0.935	584
9	73	150	0.28	0.0188	0.9803	2000	0.426	453
10	75	200	0.24	0.0195	0.9632	2000	0.300	394
11	75	250	0.21	0.0188	0.9432	2000	0.228	336
12	75	300	0.21	0.0207	0.9180	2000	0.183	306
13	74	250	0.21	0.0182	0.9432	2000	0.228	326
14	74	200	0.24	0.0185	0.9632	2000	0.300	374
15	80	150	0.28	0.0183	0.9802	2000	0.426	442
16	63	60	0.50	0.0176	0.9990	2000	1.100	605
17	64	60	0.50	0.0170	0.9990	3000	1.100	585
18	69	150	0.34	0.0189	0.9803	3000	0.426	376
19	72	200	0.28	0.0194	0.9632	3000	0.300	335
20	73	250	0.24	0.0188	0.9432	3000	0.228	294
21	75	300	0.22	0.0200	0.9180	3000	0.183	282
22	75	250	0.22	0.0185	0.9432	3000	0.228	317
23	72	200	0.24	0.0190	0.9632	3000	0.300	384
24	72	150	0.30	0.0197	0.9803	3000	0.426	445
25	70	70	0.48	0.0191	0.9980	3000	0.960	596

Cont.

Table 7, Continued

Run No.	T_a °F	T_c °F	Δp psi	w g/sec	ρ g/cc	p_c psig	μ cp	$k=\frac{14.7}{\Delta p}\times10^3\times\frac{L}{A}\times\mu\times\frac{w}{p}$
26	64	60	0.50	0.0170	0.9920	3000	1.100	585
27	72	150	0.30	0.0196	0.9803	3000	0.428	442
28	72	150	0.30	0.0196	0.9803	3000	0.426	442
29	72	250	0.22	0.0188	0.9432	3000	0.228	322
30	72	300	0.20	0.0190	0.9180	3000	0.183	294
31	72	250	0.22	0.0188	0.9432	3000	0.228	322
32	72	200	0.24	0.0183	0.9632	3000	0.300	370
33	72	150	0.30	0.0197	0.9803	3000	0.426	445
34	70	70	0.48	0.0183	0.9980	3000	0.960	572
35	70	70	0.52	0.0197	0.9980	4000	0.960	569
36	72	150	0.28	0.0174	0.9803	4000	0.426	422
37	72	200	0.25	0.0174	0.9632	4000	0.300	338
38	72	250	0.22	0.0169	0.9432	4000	0.228	290
39	72	300	0.24	0.0201	0.9180	4000	0.183	260
40	72	250	0.22	0.0165	0.9432	4000	0.228	282
41	72	200	0.25	0.0163	0.9632	4000	0.300	316
42	72	150	0.34	0.0185	0.9803	4000	0.426	369
43	75	75	0.50	0.0199	0.9954	4000	0.900	465

Table 8 Flow Data for Massillon Sandstone Core No. 4, Water Flow

Mean Pore Pressure = 300 psig

L = 5.230 cm

A = 4.866 cm^2

$$k=\frac{14.7}{\Delta p}\times 10^3 \times \frac{L}{A}\times \mu \times \frac{w}{\rho}$$

Run No.	T_a °F	T_c °F	Δp psi	w g/sec	ρ g/cc	P_c psig	μ cp	
1	70	70	0.54	0.0200	0.9980	1000	0.960	563
2	72	150	0.36	0.0207	0.9903	1000	0.426	395
3	72	200	0.32	0.0204	0.9632	1000	0.300	314
4	72	250	0.30	0.0201	0.9432	1000	0.228	266
5	72	300	0.29	0.0201	0.9180	1000	0.183	219
6	72	250	0.29	0.0192	0.9432	1000	0.228	253
7	72	200	0.31	0.0194	0.9632	1000	0.300	307
8	72	150	0.34	0.0192	0.9903	1000	0.426	399
9	75	78	0.52	0.0197	0.9969	1000	0.870	523
10	75	80	0.54	0.0204	0.9966	2000	0.850	510
11	75	150	0.36	0.0200	0.9903	2000	0.426	381
12	72	200	0.30	0.0189	0.9632	2000	0.300	310
13	72	250	0.26	0.0178	0.9432	2000	0.228	261
14	72	300	0.24	0.0170	0.9180	2000	0.183	224
15	72	250	0.26	0.0171	0.9432	2000	0.228	252
16	72	200	0.30	0.0188	0.9632	2000	0.300	308
17	72	150	0.34	0.0183	0.9903	2000	0.426	370
18	71	72	0.52	0.0196	0.9978	2000	0.935	559

Table 9 Flow Data for Massillon Sandstone Core No 5, Nitrogen Flow

p_1 = Upstream Pressure

$p_m = p_1 - 1/2\Delta p$

Confining Pressure = 1000 psig

L = 4.851 cm_2

A = 4.838 cm^2

$$k = \frac{14700 L \mu q p_a T_c}{A \Delta p p_m T_a}$$

Run No.	p_a psia	p_1 psia	Δp psi	p_m psia	$14.7/p_m$ atm^{-1}	q cc/sec	T_a ^oK	T_c ^oK	μ cp	k md
1	14.71	22.41	0.048	22.386	0.657	0.294	293	293	0.01760	1044
2	14.71	32.31	0.100	32.26	0.456	0.868	293	293	0.01760	1027
3	14.71	37.71	0.122	37.649	0.390	1.235	293	293	0.01760	1026
4	14.71	43.71	0.146	43.637	0.337	1.689	293	293	0101760	1011
5	14.71	62.71	0.202	62.609	0.235	3.289	293	293	0.01760	992
6	14.71	84.71	0.250	84.585	0.174	5.435	294.3	294.3	0.01764	983
7	14.71	110.71	0.291	110.564	0.133	8.197	294.3	294.3	0.01764	975
8	14.726	24.026	0.074	23.989	0.613	0.401	294.3	338.7	0.01959	1105
9	14.726	27.426	0.100	27.376	0.537	0.605	294.3	338.7	0.01959	1082
10	14.726	55.026	0.240	54.906	0.268	2.747	294.3	338.7	0.01959	1020
11	14.726	110.726	0.384	110.534	0.133	8.621	294.3	338.7	0.01959	993
12	14.726	30.526	0.083	30.482	0.482	0.439	295.4	394.3	0.02185	1098
13	14.726	45.726	0.156	45.648	0.322	1.185	296.5	394.3	0.02185	1050
14	14.726	65.726	0.237	65.607	0.224	2.500	296.5	394.3	0.02185	1014
15	14.726	83.726	0.285	83.583	0.176	3.846	296.5	294.3	0.02185	1018
16	14.726	110.926	0.343	110.754	0.133	6.024	296.5	394.3	0.02185	1000
17	14.726	170.73	0.550	170.45	0.0862	19.3	294.3	294.3	0.01764	788
18	14.726	218.73	0.60	218.43	0.0672	25.48	294.3	294.3	0.01764	744
19	14.726	266.73	0.63	266.41	0.0552	31.36	294.3	294.3	0.01764	715
20	14.726	331.41	0.65	331.08	0.0468	38.22	294.3	294.3	0.01764	680

Table 10. Flow Data for Massillon Sandstone Core No. 6, Nitrogen Flow

L = 5.232 cm

A = 4.866 cm^2

Run No.	P_a psia	P_1 psia	ΔP psi	P_m psia	$14.7/P_m$ atm^{-1}	q_a cc/sec	T_a °K	T_c °K	μ cp	P_c psig	$k=\frac{14700L\mu q P_a T_c}{A\Delta P P_m T_a}$ md
1	14.721	29.721	0.280	29.581	0.497	2.000	294.3	294.3	0.01764	1000	991
2	14.721	43.721	0.196	43.623	0.337	2.000	294.3	294.3	0.01764	1000	960
3	14.721	63.921	0.134	63.850	0.230	2.000	294.3	294.3	0.01764	1000	957
4	14.721	72.721	0.120	72.661	0.202	2.000	294.3	294.3	0.01764	1000	941
5	14.721	30.721	0.350	30.546	0.480	2.000	294.3	338.7	0.01959	1000	981
6	14.721	45.721	0.240	45.601	0.322	2.000	294.3	338.7	0.01959	1000	959
7	14.721	59.521	0.188	59.421	0.247	2.000	294.3	338.7	0.01959	1000	939
8	14.721	72.821	0.154	72.744	0.202	2.000	294.3	338.7	0.01959	1000	936
9	14.672	33.672	0.410	33.467	0.439	2.000	293.2	394.3	0.02185	1000	993
10	14.672	50.072	0.278	49.933	0.294	2.000	293.2	394.3	0.02185	1000	980
11	14.672	58.672	0.240	58.552	0.251	2.000	293.2	394.3	0.02185	1000	970
12	14.672	66.972	0.212	66.866	0.220	2.000	293.2	394.3	0.02185	1000	961
13	14.700	29.200	0.297	29.048	0.506	2.000	293.2	293.2	0.01760	3000	948
14	14.700	46.897	0.198	46.798	0.314	2.000	293.2	293.2	0.01760	3000	883
15	14.700	61.897	0.152	61.821	0.238	2.000	293.2	293.2	0.01760	3000	870
16	14.700	81.897	0.116	81.839	0.180	2.000	293.2	293.2	0.01760	3000	862
17	14.700	30.400	0.380	30.210	0.487	2.000	292.0	338.7	0.01959	3000	920
18	14.700	47.700	0.248	47.576	0.309	2.000	292.0	338.7	0.01959	3000	895
19	14.700	60.000	0.200	59.900	0.245	2.000	292.0	338.7	0.01959	3000	881
20	14.700	90.700	0.137	90.632	0.162	2.000	292.0	338.7	0.01959	3000	850
21	14.893	34.093	0.436	33.875	0.434	2.000	292.6	394.3	0.02185	3000	939
22	14.893	51.693	0.295	51.546	0.285	2.000	292.6	394.3	0.02185	3000	912
23	14.893	74.193	0.210	74.088	0.198	2.000	292.6	394.3	0.02185	3000	890
24	14.893	86.893	0.180	86.803	0.169	2 000	292.6	394.3	0.02185	3000	887
25	14.893	92.593	0.170	92.508	0.159	2 000	292.6	394.3	0.02185	3000	881

Cont

Table 10, continued

Run No	p_a psia	p_l psia	Δp psi	p_m psia	$14.7/p_m$ atm^{-1}	a cc sec	T_a ^oK	T_c ^oK	μ cp	p_c psig	$k=\frac{14700L\mu q p_a T_c}{A\Delta p p_m T_a}$ md
26	14.893	32.761	0.293	32.614	0.451	2.000	292.0	294.8	0.1767	4000	871
27	14.893	50.761	0.190	50.666	0.290	2.000	292.0	294.8	0.01767	4000	865
28	14.893	62.761	0.156	62.683	0.235	2.000	292.0	294.8	0.01767	4000	851
29	14.893	81.961	0.121	81.900	0.180	2.000	292.0	294.8	0.01767	4000	840
30	14.893	34.260	0.355	34.083	0.431	2.000	292.0	338.7	0.01959	4000	876
31	14.893	49.56	0.248	49.436	0.297	2.000	292.0	338.7	0.01959	4000	865
32	14.893	63.160	0.198	63.061	0.233	2.000	292.0	338.7	0.01959	4000	849
33	14.893	81.060	0.156	80.982	0.182	2.000	292.0	338.7	0.01959	4000	839
34	14.893	90.56	8.140	90.4	0.162	2.000	292.0	338.7	0.01959	4000	836
35	14.893	35.447	0.450	35.222	0.417	2.000	289.8	394.3	0.02185	4000	886
36	14.893	49.947	0.320	49.787	0.295	2.000	289.8	394.3	0.02185	4000	882
37	14.893	61.847	0.261	61.717	0.238	2.000	289.8	394.3	0.02185	4000	872
38	14.893	77.747	0.210	77.643	0.189	2.000	289.8	394.3	0.02185	4000	861

Table 11. Flow Data for Massillon Sandstone Core No. 0, Oil Flow

Mean Pore Pressure = 200 psig

L = 4.961 cm

A = 4.866 cm^2

$$k = \frac{14.7}{\Delta p} \times 10^3 \left(\frac{L \mu w}{A \rho} \right)$$

Run No	T_a °F	T_c °F	Δp psi	w g/sec	ρ g/cc	p_c psig	μ cp	md
1	66	63	4.04	0.00525	0.84985	1000	37.40	857
2	68	103	3.39	0.01299	0.83641	1000	13.38	780
3	66	153	3.05	0.0330	0.81980	1000	5.50	839
4	60	200	3.37	0.0573	0.80458	1000	2.98	800
5	65	250	4.30	0.09091	0.78859	1000	1.85	799
6	70	200	3.08	0.05774	0.80458	1000	2.98	805
7	70	150	4.00	0.03119	0.82083	1000	5.66	805
8	73	100	3.39	0.01268	0.83743	1000	14.15	805
9	68	70	4.00	0.006494	0.84747	1000	30.51	876
10	68	70	4.30	0.006423	0.84747	2000	30.51	866
11	68	150	4.00	0.03077	0.82083	2000	5.66	795
12	68	200	4.00	0.05682	0.80458	2000	2.98	788
13	70	250	4.00	0.09091	0.78859	2000	1.85	799
14	72	200	4.00	0.05599	0.80458	2000	2.98	777
15	72	150	4.00	0.02960	0.82083	2000	5.66	765
16	70	76	4.00	0.007205	0.84542	2000	25.80	824
17	70	75	4.00	0.00626	0.84577	4000	26.2	726
18	62	150	4.00	0.02747	0.82083	4000	5.66	710
19	64	200	4.00	0.04985	0.80458	4000	2.98	692
20	68	250	4.00	0.07813	0.78859	4000	1.85	689
21	68	197	4.00	0.04708	0.80552	4000	3.06	671
22	68	150	4.00	0.02573	0.82083	4000	5.66	665
23	68	72	4.00	0.005274	0.84679	4000	28.79	672

Table 12 Flow Data for Massillon Sandstone Core No. 11, Oil Flow

Mean Pore Pressure = 200 psig

L = 4.980 cm_2
A = 4.866 cm^2

$$k=\frac{14.7}{\Delta p}x10^3x\frac{L\mu w}{A\rho}$$

Run No.	T_a °F	T_c °F	Δp psi	w g/sec	ρ 1g/cc	P_c psig	μ cp	md
1	67	67	4.00	0.00652	0.84849	1000	33.5	960
2	67	150	4.00	0.0344	0.82083	1000	5.66	885
3	68	225	4.00	0.07899	0.7965	1000	2.30	851
4	69	295	4.00	0.13755	0.77446	1000	1.30	861
5	69	225	4.00	0.078864	0.7965	1000	2.30	850
6	71	71	4.00	0.00733	0.84713	1000	29.65	957
7	71	71	4.0	0.00690	0.84712	3000	29.65	899
8	72	150	4.0	0.0332	0.82083	3000	5.66	854
9	73	225	4.0	0.0742	0.7965	3000	2.30	799
10	73	300	4.0	0.1253	0.7729	3000	1.28	774
11	72	225	4.00	0.0699	0.7965	3000	2.30	753
12	65	66	4.00	0.00538	0.84883	3000	34.80	822

Table 13 Flow Data for Unconsolidated Ottawa Silica Sand #14, Water Flow

Mean Pore Pressure = 200 psi

L = 5.696 cm

A = 5.067 cm^2

Average Grain Size Diameter = 0.385 mm

Run No.	T_a °F	T_c °F	p psi	w g/sec	g/cc	P_c psig	μ cp	$k=\frac{14.7}{\Delta p}x10^{3}x\frac{L\mu w}{A\rho}$ md
1	61	61	0.040	0.0494	0.9990	500	1.100	22,464
2	64	150	0.020	0.0517	0.9803	500	0.426	18,544
3	68	225	0.007	0.256	0.9532	500	0.260	16,510
4	69	300	0.005	0.0185	0.9180	500	0.183	12,200
5	62	62	0.053	0.0652	0.9989	1000	1.070	21,776
6	66	150	0.027	0.0645	0.9803	1000	0.426	17,155
7	68	225	0.010	0.0296	0.9532	1000	0.260	13,355
8	71	300	0.022	0.0625	0.9180	1000	0.183	9,359
9	64	64	0.023	0.0244	0.9987	1500	1.050	18,431
10	68	150	0.031	0.0645	0.9803	1500	0.426	14,945
11	68	225	0.034	0.0678	0.9532	1500	0.260	8,988
12	72	300	0.026	0.0513	0.9180	1500	0.183	6,497

Table 14 Flow Data for Unconsolidated Ottawa Silica Sand Core No. 15, Water Flow

Mean Pore Pressure = 200 psig

L = 5.59 cm

A = 5.067 cm^2

Average Grain Size Diameter = 0.156 mm

Run No.	T_a °F	T_c °F	Δp psi	w g/sec	ρ g/cc	P_c psig	μ cp	$k=\frac{14.7\times10^3}{\Delta p}\frac{L\mu w}{A}$ md
1	62	62	0.063	0.0336	0.9989	500	1.07	9265
2	70	150	0.068	0.060	0.9803	5500	0.426	5900
3	72	225	0.079	0.0820	0.9532	500	0.260	4588
4	68	300	0.035	0.0323	0.9180	500	0.183	2979
5	70	225	0.077	0.0820	0.9532	500	0.260	4707
6	72	150	0.088	0.732	0.9803	500	0.426	5860
7	66	65	0.063	0.0278	0.9986	500	1.030	7372
8	66	150	0.069	0.040	0.9803	500	0.426	5569
9	72	225	0.090	0.0909	0.9532	500	0.260	4467
10	72	300	0.040	0.0357	0.9180	500	0.183	2885
11	72	225	0.050	0.050	0.9532	500	0.260	4422
12	72	150	0.055	0.435	0.9803	500	0.426	5569
13	68	68	0.068	0.0328	0.9982	500	0.990	7752
14	68	68	0.062	0.0279	0.9982	1000	0.990	7203
15	72	150	0.066	0.536	0.9803	1000	0.426	5718
16	72	225	0.008	0.00752	0.9532	1000	0.260	4125
17	72	300	0.033	0.0244	0.9180	1000	0.183	2388
18	68	68	0.062	0.0270	0.9982	1000	0.990	7009
19	70	70	0.100	0.0333	0.9980	2000	0.960	5197
20	70	150	0.080	0.0469	0.9803	2000	0.426	4127
21	70	225	0.057	0.0374	0.9532	2000	0.260	2900
22	66	300	0.090	0.0531	0.9180	2000	0.183	1907
23	68	225	0.045	0.0290	0.9532	2000	0.260	2850
24	68	150	0.078	0.044	0.9803	2000	0.426	3985
25	72	72	0.077	0.0238	0.9978	2000	0.940	4722

Table 15 Fl Data for Unconsolidated Ottawa Silica Sand Core No 16, Nitrogen and Water Flow

L = 5.657 cm

A = 5.067 cm^2

Average Grain Size Diameter = 0.156 mm

$$k = \frac{14.700 L \mu q_a p_a T_c}{A \Delta p p_m T_a}$$

Run No.	p_a psia	p_1 psia	Δp psi	p_m psia	$14.7/p_m$ atm^{-1}	q_a cc/sec	T_a °K	T_c °K	μ cp	p_c psig	k md
1	14.648	30.648	0.012	30.641	0.480	0.455	290.9	290.9	0.01746	2000	5194
2	14.648	45.648	0.021	45.638	0.322	1.124	290.9	290.9	0.01746	2000	4921
3	14.648	53.848	0.026	53.835	0.273	1.587	290.9	290.9	0.01746	2000	4760
4	14.648	61.948	0.030	61.933	0.237	2.105	290.9	290.9	0.01746	2000	4756
5	14.648	72.948	0.035	72.930	0.202	2.830	290.9	290.9	0.01746	2000	4653
6	14.810	42.810	0.026	42.798	0.343	0.930	289.8	338.7	0.01959	2000	4978
7	14.648	53.948	0.033	53.931	0.273	1.563	289.8	338.7	0.01959	2000	4832
8	14.648	63.148	0.038	63.129	0.233	2.083	289.8	338.7	0.01959	2000	4780
9	14.648	71.848	0.044	71.826	0.205	2.679	289.8	338.7	0.01959	2000	4665
10	14.736	34.036	0.022	34.025	0.432	0.561	289.8	394.3	0.02185	2000	5386
11	14.736	41.736	0.029	41.722	0.352	0.870	289.8	394.3	0.02185	2000	5176
12	14.736	52.736	0.039	52.717	0.279	1.429	289.8	394.3	0.02185	2000	4996
13	14.736	61.736	0.047	61.693	0.238	1.970	289.8	394.3	0.02185	2000	4886

Water Flow

$$k = \frac{14.7 \times 10^3 \times L \mu w}{A \Delta p \rho}$$

Run No	T_a °F	T_c °F	Δp psi	w g/sec	ρ g/cc	p_c psig	μ cp	k md
14	62	62	0.06	0.007	.9989	2000	1.07	2127

Table 16 Flow Data for Unconsolidated Ottawa Silica Sand Core No 17, 2-Octanol Flow

Mean Pore Pressure = 200 psig

L = 5.894 cm

A = 5.067 cm^2

Average Grain Size Diameter = 0.156 mm

$$k = \frac{14.7 \times 10^3}{\Delta p} \frac{L \mu w}{A \rho}$$

Run No.	T_a °F	T_c °F	Δp psi	w g/sec	ρ g/cc	P_c psig	μ cp	k md
1	66	66	0.697	0.0318	0.8200	500	10.58	10049
2	64	150	0.100	0.0198	0.7868	500	2.30≈	9924
3	68	225	0.100	0.0443	0.7573	500	1.04	10390
4	72	300	0.120	0.0862	0.7280	500	0.61	10291
5	72	225	0.095	0.0403	0.7573	500	1.04	9954
6	69	150	0.080	0.0161	0.7868	500	2.306	10104
7	64	65	0.450	0.0185	0.8203	500	10.75	9222
8	65	65	0.700	0.0278	0.8203	1000	10.75	8893
9	68	150	0.105	0.01905	0.7868	1000	2.306	9101
10	70	225	0.099	0.0375	0.7573	1000	1.04	8895
11	70	300	0.110	0.0722	0.7280	1000	0.61	9404
12	70	225	0.100	0.0385	0.7573	1000	1.04	9032
13	72	150	0.100	0.0171	0.7868	1000	2.30≈	8567
14	70	72	0.44	0.0205	0.8180	1000	8.60	8364
15	70	72	0.62	0.0247	0.8180	2000	8.60	7160
16	68	150	0.220	0.0354	0.7868	2000	2.30≈	8064
17	72	225	0.220	0.0769	0.7573	2000	1.04	8211
18	76	300	0.100	0.0577	0.7280	2000	0.61	8266
19	74	225	0.085	0.0292	0.7573	2000	1.04	8066
20	74	150	0.170	0.0230	0.7868	2000	2.30≈	7657
21	70	70	0.620	0.0206	0.8182	2000	9.10	6325

9.2 Core Data

CORE DATA

9 2-1 Consolidated Massillion Sandstone Cores

9.2-1-1 Physical Properties

	[illegible]	[illegible]	[illegible]	5	6	[illegible]	9	10	11	12
Length, cm	5.233	5.187	5.230	4.851	5.232	4.770	4.953	4.961	4.940	4.9[illegible]
Diameter, cm	2.482	2.497	2.489	2.482	2.489	2.489	2.489	2.489	2.489	2.489
Dry Weight, gm	51.4320	51.1464	51.7055	49.1466	51.0554	46.4438	48.4028	48.7000	48.2646	48.562
Wet Weight, gm	56.9464	56.8586	56.4000	54 [illegible]000	49.1483					
Porosity, % Bulk Volume	21.8	22 5	22 4	z3 2	22	22	22	z2	2z	z2

9.2-1-2 Mineralogical Co [illegible]ition

	Weight %
Silicon dioxide	[illegible]5.0[illegible]
Aluminum oxide	2.7[illegible]
Iron oxide	0.6
Calcium oxide	0.3
Magnesium oxide	0.25

9.2-1-3 Description: The Massillon sandstone is found in Holmes County, Ohio, and has been extensively quarried for a variety of purposes. The stone is medium-to-coarse grained and is composed mostly of quartz grains, which are subangular to subrounded in shape. The cementing materials are iron oxide, clay minerals, and secondary silica.

Tests made for the Briar Hill Stone Company show that the stone has an absorption of water of approximately 6% by weight. The crushing strength ranges from 4000 to 6000 psi, 5000 psi being about average. The stone weighs 135 pounds per cubic foot. The average permeability of the samples used in this study was 800 md, and the average porosity about 22%.

9.2-2 Unconsolidated Ottawa Silica

9.2-2-1 Physical Properties

Core No.	14	15	16	17
Length, cm	5.696	5.590	5.657	5.894
Cross-Sectional Area, cm^2	5.067	5.067	5.067	5.067
Average Grain Size, mm	(35-45 mesh)	(80-100 mesh)	(80-100 mesh)	(80-100 mesh)

9.2.2-2 Mineralogical Composition

	Weight %
Silicon dioxide (SiO_2)	99.806
Aluminum oxide (Al_2O_3)	0.047
Iron oxide (Fe_2O_3)	0.019
Titanium dioxide (TiO_2)	0.018
Calcium oxide (CaO)	<0.01
Magnesium oxide (MgO)	<0.01
Loss on Ignition (LOI)	0.09

9.2-2-3 Description: The Ottawa sand used in this study is the No. 17 silica grade and is commercially available from the Ottawa Division, Parker Industrial and Foundry Supply, Burlingame, California. It is more than 99% weight quartz and the grains are fairly well rounded. The distribution of grain sizes is as follows:

U.S. Sieve No.	Opening, Millimeter	Percent Weight Retained
40	0.420	8.1
50	0.297	44.5
70	0.210	28.8
100	0.149	12.7
140	0.105	4.4
200	0.074	1.1
270	0.053	0.2

The sand was sieved and only uniformly sized grains were used to prepare a core for this study.

9.3 Derivation of Equations

9.3-1 Capillary Tube Viscometer: Because liquid viscosity data obtained from suppliers are average product quantities and those from conventional references were not given at high working temperatures, it was necessary to determine viscosity versus temperature at operating pressures.

A capillary tube viscometer, whose overall length was 62.875 inches and whose internal diameter was 0.033 inches, was constructed from a 316 stainless steel tube. The linear coefficient of thermal expansion was 8.9 $\times 10^{-6}$ in/in-°F.

The laminar flow of liquids through circular conduits obeys Poiseuille's law:

$$q = \frac{\pi r^4 \Delta p}{8 \mu \ell} \qquad (9\text{-}1)$$

where q = flow rate, cc/sec; r = inside radius, cm; Δp = pressure drop, dynes/cm2; μ = liquid viscosity, poises, ℓ = length of capillary, cm.

For r and ℓ in inches, Δp in psi, and μ in cp units, Eq. 9-1 becomes:

$$q = 4.437 \times 10^7 \frac{r^4 \Delta p}{\ell \mu} \qquad (9\text{-}2)$$

and

$$\mu = 0.5230 \frac{\Delta p}{q} \qquad (9\text{-}3)$$

Knowing the actual value of viscosity at 70°F, and from measurements of p and q, the multiplying constant was found to be 0.5113. Therefore:

$$\mu_{70} = 0.05113 \frac{\Delta p}{q} \qquad (9\text{-}4)$$

Therefore, a graph of $Y = \frac{p_m \Delta p \left(1+\frac{b}{p_m}\right)}{\mu \bar{z} \frac{L}{A} \frac{T}{T_a} p_a q_a}$ vs. $X = \frac{a}{A\mu}\left(1+\frac{b}{p_m}\right)$

should yield a straight line of slope β and intercept $\frac{1}{k}$, provided that the value of **b** is known.

Eq. 9-10 was the working equation for this apparatus. The results agree closely with those found in the International Critical Tables.[39]

9.3-2 Visco-Inertial Flow of Gas: The quadratic equation as proposed by Forchheimer and modified by Cornell and Katz (see refs. 10 and 11) is:

$$-\frac{dp}{dL} = \alpha\mu q + \beta\rho q^2 \qquad (9\text{-}11)$$

for the case of visco-inertial flow of gas. For viscous flow, the quadratic term of 9-11 is small enough to be neglected, and a has to be the reciprocal of permeability, i.e., $\alpha = 1/k$.

The integrated form of Eq. 9-11 for horizontal linear flow in the absence of slippage is:

$$\frac{p_m \Delta p}{\mu z \frac{L}{A}\frac{T}{T_a} p_a q_a} = \alpha + \beta \frac{\rho}{A}\frac{q}{\mu} \qquad (9\text{-}12)$$

When there is gas slippage, α becomes $\frac{1}{k(1+\frac{b}{p_m})}$. Replacing α by $\frac{1}{k(1+\frac{b}{p_m})}$ and simplifying,

$$\frac{p_m \Delta p (1+\frac{b}{p_m})}{\mu z \frac{L}{A}\frac{T}{T_a} p_a q_a} = \frac{1}{k} + \frac{\beta\rho q}{A\mu}(1 + \frac{b}{p_m}) \qquad (9\text{-}13)$$

or

$$Y = \frac{1}{k} + \beta X \qquad (9\text{-}14)$$

At temperatures, T, other than room temperature, the length of the tube is:

$$\ell_T = \ell_{70}\left[1 + B\ (T-70)\right] \qquad (9\text{-}5)$$

and

$$r_{T4} = r_{70}^4\left[1 + B\ (T-70)\right]^4 \qquad (9\text{-}6)$$

or

$$\frac{r_T^4}{\ell_T} = \frac{r_{70}^4}{\ell_{70}}\left[1 + B\ (T-70)\right]^3 \qquad (9\text{-}7)$$

Because B, the linear coefficient of thermal expansion, is small, Eq. 9-7 can be approximated as:

$$\frac{r_T^4}{\ell_T} = \frac{r_{70}^4}{\ell_{70}}\left[1 + 3B\ (T-70)\right] \qquad (9\text{-}8)$$

For the apparatus:

$$\mu_T = 0.05113\left[1 + 2.67 \times 10^{-5}\ (T-70)\right]\frac{\Delta p}{q} \qquad (9\text{-}9)$$

Therefore, the viscosity at any temperature is:

$$\mu_T = \alpha_T \frac{\Delta p}{q} \qquad (9\text{-}10)$$

Where: $\alpha_T = 0.05113\left[1 + 2.67 \times 10^{-5}\ (T-70)\right]$

9.4 List of Manufacturers

LIST OF MANUFACTURERS

The following is a list of the various pieces of equipment or supplies that were used in this work, together with the corresponding names of manufacturers and/or suppliers from whom they were acquired.

Chevron White Mineral Oil No. 3 - Van Waters E Rogers, Inc. San Francisco.

Pressure Transducers - Dynasciences Corp., Model KP 15, c/o Gaco Instrument Sales, 655 Castro Street, Suite 2, Mountain View, Ca., 94040 (961-2222).

Barnett Industrial Dead Weight Tester - c/o Gaco Instrument Sales, 655 Castro Street, Suite 2, Mountain View, Ca., 94040 (961-2222).

Pressure Indicator - Pace Model CD 25, c/o Gaco Instrument Sales, 655 Castro Street, Suite 2, Mountain View, Ca., 94040 (961-2222).

Pressure Regulator - Volumetrics, Model VRC-400, 1025 Arbor Vitae Street, Inglewood, Ca., 90301 (213) 641-3747, or c/o Gaco Instrument Sales, 655 Castro Street, Suite 2, Fountain View, Ca., 94040 (961-2222).

High Pressure Regulator - Model 4-580, Matheson Gas Products, Newark, Ca. (793-2559).

Variable Rate Oil Pump - Model PC, Whitey Tool E Die Company, 5679 Landregan Emvl., Oakland, Ca, (653-5100), loan from USBM.

Hydraulic Hand Pump - Enerpac, Model P-39, Paul Monroc Hydraulics, Inc., 1570 Gilbreth Road, Burlingame, Ca., 94010 (697-2950).

Constant Rate Pump - Hand-made equivalent to Ruska 2200 series. Uses Viton 0 ring with machined teflon back-up ring.

Accumulators (Greerolator), Model No. 20-30 TMR-S-½ WS, Hydraulic Controls, Inc., 1330 6th St., Emeryville, Ca., 94608 (658-8300).

Recording Potentiometer (for temperature) - Model Speedo Max W, Leeds E Northrup, 1095 Market St., San Francisco, Ca. (349-6656).

Thermocouples - Iron-Constantan, Conax, c/o Instrument Laboratory, 644 Emerson St., Palo Alto, Ca., 94303 (328-1040).

Temperature Controller - API Model 228 with 4010 Power Pack, API Instruments, 2339 Charleston Rd., Mountain View, Ca., 94040 (964-0512).

Laboratory Flowrator Kit - Model No. 10A3565ALKZ, Fisher E Porter Co., 1341 North Main St., Walnut Creek, Ca., 94596 (933-8880).

Core Sleeve - Viton A tubing, West American Rubber Co., 750 North Main St., Orange, Ca., 92668 (714-532-3355).

O Rings - Viton A with teflon back-up rings, ABSCOA Industries, 880 Burlingame Ave., Redwood City, Ca. (369-4897) or 1071 W. Arbor Vitae St., Inglewood, Ca., (213-7764561).

Tubing - Tubesales, 500 Sansome St., San Francisco, Ca. (EN-1-1919).

Fittings E Valves - Van Dyke E Fitting Co., 5525 Marshal St., Oakland, Ca. (658-1700).

Gas Analyzer - Gas Master, Laboratory Model, GOW-MAC Instrument Co., 100 Kings Rd., Madison, N.J. 07940 (201-377-3450) or Applied Instrument Co., 199 1st Street, Los Altos (941-5928).

Recording Potentiometer (for pressure) - Two pen multi-range recorder, Leeds and Northrup, BD-9, P.O. Box 634, Belmont, Ca. (593-8392).

Alundum Core - Norton Co., ICD, 2555 Layafette St., Santa Clara, Ca. 95050 (234-7710).

Lapp Pulsafeeder Pump - Model LS-20, 316SS, 1/6 hp, 94 Natoma St., San Francisco, Ca. 94105 (391-7650).

Ottawa Silica, No. 17 Silica, Parker Industrial and Foundry Supply, 1881 Rolling Rd., Burlingame, Ca., 94010 (697-8865).

Massillon Sandstone - The Briar Hill Stone Co., Glenmont, Ohio, 44628 (216-2764011).

10. NOMENCLATURE

English

A = area, cm^2

k = permeability, md

L = length of core, cm

p = pressure, psi

q = flow rate, cc/sec

w = flow rate, gm/sec

T = temperature, oK or ^oF

r = radius, cm

v = flow velocity, cm/sec

Greek

ρ = density, gm/cc

μ = viscosity, cp

ϕ = porosity, fraction

Δ = increment

Subscripts

a = atmospheric condition

c = core or confining

m = mean value

T = temperature